AD-A151 421 TRANSFORMATION TOUGHENED CERAMICS A POTENTIAL MATERIAL FOR LIGHT DIESEL E..(U) MICHIGAN UNIV ANN ARBOR DEPT OF MATERIALS AND METALLURGICAL E.. T Y TIEN JUN 84 1/1

UNCLASSIFIED ARMRC-TR-84-46 DAAG46-84-K-0001 F/G 11/2 NL

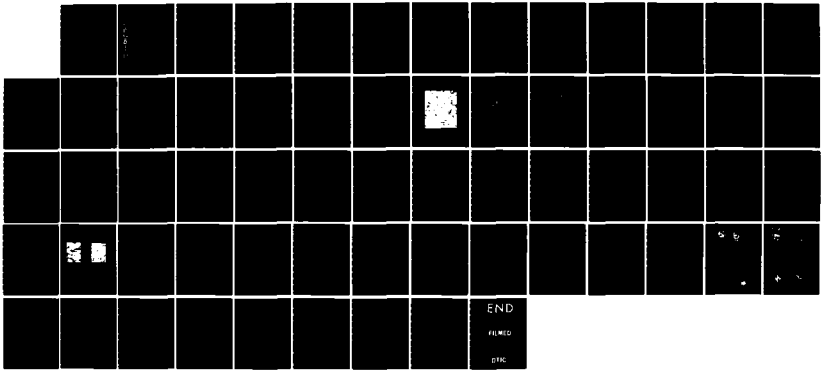

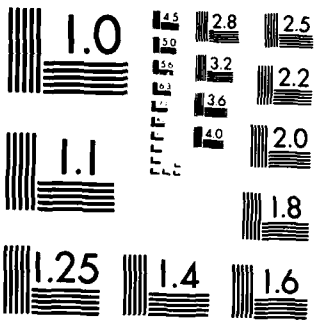

ENERGY

DOE/ER/10107

AMMRC TR 84-46

Transformation Toughened Ceramics - A Potential Material for Light Diesel Engine Application

T. Y. Tien
Materials and Metallurgical Engineering
The University of Michigan
Ann Arbor, Michigan 48109

June 1984

Semi-annual Report - for Period
Oct. 1, 1983 - March 31, 1984

Contract No. DAAG46-84-K-0001

Prepared for
Army Materials and Mechanics Research Center
Watertown, Massachusetts 02172

Under AMMRC/DOE Interagency Agreement DE-A101-77CS51017
Department of Energy
Office of Vehicle and Engine Research and Development
Ceramic Technology for Advanced Heat Engines Programs

U. S. Department of Energy
Division of Transportation Energy Conservation

The findings in this report are not to be construed as an official Department of the Army position, unless so designated by other authorized documents.

Mention of any trade names or manufacturers in this report shall not be construed as advertising nor as an official indorsement or approval of such products or companies by the United States Government.

DISPOSITION INSTRUCTIONS

Destroy this report when it is no longer needed.
Do not return it to the originator.

UNCLASSIFIED

SECURITY CLASSIFICATION OF THIS PAGE (When Data Entered)

REPORT DOCUMENTATION PAGE		READ INSTRUCTIONS BEFORE COMPLETING FORM
1. REPORT NUMBER AMMRC TR 84-46	2. GOVT ACCESSION NO. AD-A151 421	3. RECIPIENT'S CATALOG NUMBER
4. TITLE (and Subtitle) Transformation Toughened Ceramics - A Potential Material for Light Diesel Engine Application		5. TYPE OF REPORT & PERIOD COVERED 6. PERFORMING ORG. REPORT NUMBER
7. AUTHOR(s) T. Y. Tien		8. CONTRACT OR GRANT NUMBER(s) DAAG46-84-0001
9. PERFORMING ORGANIZATION NAME AND ADDRESS The University of Michigan Ann Arbor, Michigan 48109		10. PROGRAM ELEMENT, PROJECT, TASK AREA & WORK UNIT NUMBERS
11. CONTROLLING OFFICE NAME AND ADDRESS Army Material and Mechanics Research Center Watertown, Massachusetts 02172		12. REPORT DATE June 1984 13. NUMBER OF PAGES 54
14. MONITORING AGENCY NAME & ADDRESS(if different from Controlling Office)		15. SECURITY CLASS (of this report) Unclassified 15a. DECLASSIFICATION/DOWNGRADING SCHEDULE

16. DISTRIBUTION STATEMENT (of this Report)

Approved for public release; distribution unlimited.

17. DISTRIBUTION STATEMENT (of the abstract entered in Block 20, if different from Report)

18. SUPPLEMENTARY NOTES

19. KEY WORDS (Continue on reverse side if necessary and identify by block number)

Alumina, Zirconia, Toughened Ceramics, Ceramics, Fracture Toughness, Processing, Microstructure, Mullite.

20. ABSTRACT (Continue on reverse side if necessary and identify by block number)

This report contains three parts: The mechanical behavior of composites in the system Al_2O_3:Cr_2O_3/ZrO_2:HfO_2 are presented in the first part. The thermal conductivity studies of these compositions will be presented in the second part. The mullite - ZrO_2 system will be discussed in the third part. The results indicate that a composition containing 15 mole % of Cr_2O_3 in the matrix phase has a thermal conductivity comparable to that of stabilized zirconia. Composites heat treated at 900° and 1200°C for 400 hours showed no degradation in mechanical properties.

DD FORM 1 JAN 73 1473 EDITION OF 1 NOV 65 IS OBSOLETE

UNCLASSIFIED

SECURITY CLASSIFICATION OF THIS PAGE (When Data Entered)

Partially stabilized zirconia (PSZ), containing one of several stabilizers, has been considered as a leading candidate for application in advanced heat engines. Properties which are particularly attractive are high toughness, high coefficient of thermal expansion (approaching that of metals) and low thermal conductivity. There are indications, however, that the stability of this material is low at elevated temperatures and that, at temperatures as low as 650°C in magnesium partially stabilized zirconia, a thermally activated process causes a eutectoid decomposition which produces monoclinic ZrO_2 and MgO resulting in severe degradation of strength. Furthermore, additions of stabilizing oxides, e.g. MgO, CaO, Y_2O_3, CeO_2 etc. result in a decrease in the equilibrium tetragonal-monoclinic transformation temperature below that of pure ZrO_2 ($\sim$ 1150°C) thus limiting the usefulness of stress induced transformation toughening and decreasing the incremental toughening effect with increasing temperature. PSZ, therefore, appears unable to meet the requirement of long term stability and high temperature strength and toughness.

Tetragonal zirconia (TZP) share many of the advantages and disadvantages of PSZ type materials. Strengths in excess of 2.5 GPa have been measured but the room temperature fracture toughness seldom exceeds 6 $MNm^{-3/2}$. TZP materials also exhibit a time dependent strength degradation particularly in water vapor containing atmospheres, at temperatures of $\sim$ 250°C. This degradation is poorly understood but seems characteristic of this class of materials. Furthermore, the very fine grain sizes which are required are expected to result in poor creep resistance at elevated temperatures. As in PSZ, the stabilizing agents are expected to decrease the magnitude of the transformational chemical free energy change thus limiting the degree of transformation toughening. For these reasons, TZP materials are believed to be incapable of meeting the materials requirements for heat engine applications.

Alumina-zirconia composites have been reported to have a high toughness (> 8 $MNm^{-3/2}$) and high strength (>1000 MPa) at room temperature. These composites, however, have a relatively high thermal conductivity at room temperature, decreasing with increasing temperatures. In order to modify this behavior, solid solution additives, such as Cr_2O_3, can be utilized, resulting in a decrease of $\sim 60\%$ in the thermal conductivity at room temperature. Accompanying this large decrease in thermal conductivity is a small increase in modulus of elasticity and hardness which is also expected to be effective at high temperatures in reducing matrix creep.

High temperature mechanical properties of Al_2O_3 - ZrO_2 composites have been disappointing, with significant decreases in fracture toughness of Al_2O_3 - ZrO_2 containing 2 mole % Y_2O_3 composites at temperatures as low as 600°C. This decrease is a direct result of the increasing stability of the matastable retained tetragonal particles. Thus, the transformation toughening decreases as the test temperature approaches the equilibrium temperature. This situation is aggravated by the addition of stabilizing agents, such as Y_2O_3. Addition of HfO_2 to ZrO_2 has the effect of raising the tetragonal-monoclinic transformation temperature from ~ 1170°C for pure ZrO_2 to ~ 1620°C for pure HfO_2. Pure HfO_2, in spite of its promising high temperature performance, cannot be utilized for practical reasons: 1) the critical particle size for spontaneous transformation to monoclinic upon cooling is believed to be less than that achievable by conventional processing techniques and 2) in order for the HfO_2 particle to attain the tetragonal symmetry, temperatures in the tetragonal phase must be reached during fabrication. These very high temperatures would result in very rapid growth of the matrix grains as well as the HfO_2 particles, resulting in a body with a low retained tetragonal fraction and poor mechanical

properties. Because ZrO_2 and HfO_2 form continuous solid solution, thus, there must be compositions in this solid solution series which will be suitable for this particular application.

In seemed that some compositions in the system Al_2O_3:Cr_2O_3/ZrO_2:HfO_2 may offer an opportunity to provide an alternative material for heat engine applications. This investigation was then initiated. Some of the results were given in this report.

This report contains three parts. The first part reports the progress in the Al_2O_3-Cr_2O_3-ZrO_2-HfO_2 system. The second part of this report presents the thermal diffusivity and conductivity measurements by laser flash method. The third part reports the results in the mullite system. The accomplishments during the last reporting period are summarized in the followings and the reports are attached as Appendices.

1. Transformation Toughening in the Al_2O_3-Cr_2O_3-ZrO_2-HfO_2 System:

Pre-reacted Al_2O_3-Cr_2O_3 solid solution powders of the matrix material and ZrO_2-HfO_2 solid solution powders of the dispersed phase were attrition milled to sub-micron sizes. These milled powders were then mixed in a ball mill, dried and isostatically pressed. The pressed specimens were then sintered at 1550°C for two hours under low oxygen partial pressures in an induction furnace with a graphite suscepter. The densities of these sintered specimens were found to be >98% of the theoretical with an average grain size <5μm and dispersed particle size <1μm. Toughness of these samples were measured by indentation method and were found to have a maximum (about 6 $MPaM^{\frac{1}{2}}$) at room temperature for composites containing 10 mole % of HfO_2. Specimens aged at 1200° and 900°C for 400 hours showed no toughness and no microstructure changes.

2. Thermal diffusivity and conductivity measurements:

Thermal diffusivity of composites in this system Al_2O_3-Cr_2O_3-ZrO_2-HfO_2 were measured by the laser flash method. Thermal conductivities of some compositions were calculated using the published specific heat data. The results of these measurements confirmed the results reported earlier measured by comparison method. Composites with high Cr_2O_3 (>20 mole %) contents showed thermal conductivity values lower than that of PSZ at temperatures higher than

400°C. Comparison of the conductivities of these composites with that of PSZ are given in Fig. 1. This work was done in collaboration with Professor Hasselman of Virginia Polytechnic Institute of Technology.

3. The Mullite system:

Compositions of mullite containing 15 volume % of the dispersed ZrO_2 solid solution particles containing 0, 10 and 20 mole % HfO_2 were prepared by sol-gel method. The Calcined powders of these compositions were sintered in air at 1550° and 1600°C for different lengths of time. Specimens with different grain size and different dispersed particle size were obtained. A maximum toughness value was observed for specimens with a dispersed particle size (critical particle size) about 0.3 μm. Because of the scatterness of the data points, it was not possible to delineate the effect of the HfO_2 content on the toughening effect of the ceramics and the critical particle size of the dispersed phase as a function of the HfO_2 content.

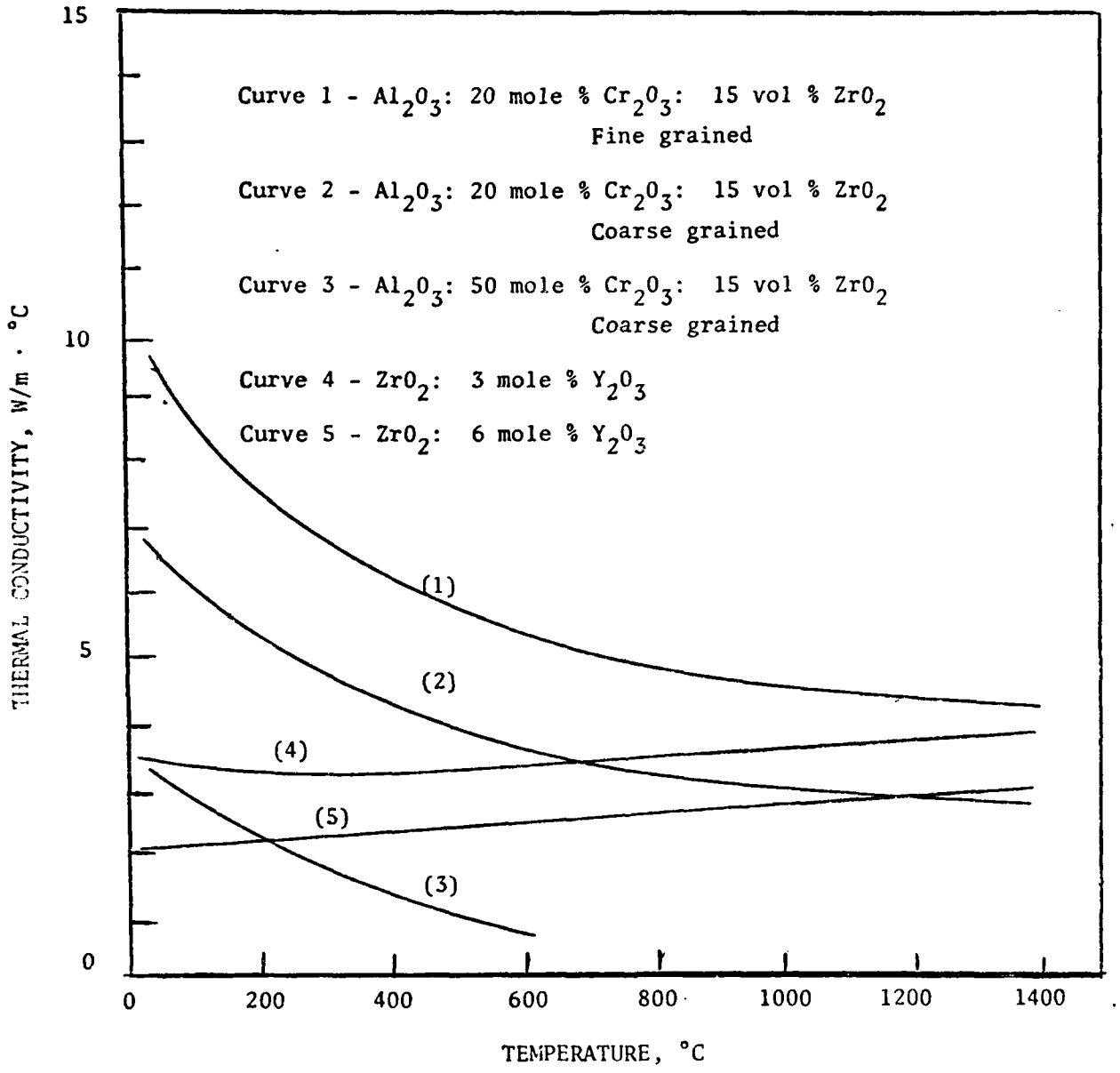

Figure 1. Thermal Conductivity of compositions in the system Al_2O_3 = Cr_2O_3 / ZrO_2 : HfO_2.

Appendix A

Transformation Toughening in the Al_2O_3-Cr_2O_3-ZrO_2-HfO_2 System

by

T. K. Brog, J. W. Jones and T. Y. Tien
Materials and Metallurgical Engineering Deptartment
The University of Michigan
Ann Arbor, Michigan 48109

ABSTRACT

The effect of dispersed phase composition and volume fraction on fracture toughness of Al_2O_3-Cr_2O_3/ZrO_2-HfO_2 composites has been investigated. For samples containing 0 and 10m/o HfO_2 in ZrO_2, the maximum fracture toughness occurred at 10v/o dispersed phase. No clearly defined toughness peak was observed for the samples containing 30m/o HfO_2 in the dispersed phase and the maximum toughness was considerably lower than those observed for sample lower HfO_2 contents.

The fraction of ZrO_2-HfO_2 particles which were retained in the tetragonal symmetry in the as-sintered and in the as-ground condition decreased with increasing volume fraction of dispersed phase and with increasing HfO_2 content. Preliminary results indicate that thermal exposure at 1200°C for times as long as 300 hours caused no measurable change in the fracture toughness or in the retained tetragonal phase content.

MATERIALS AND EXPERIMENTAL PROCEDURE

Solid solutions of Al_2O_3-5m/oCr_2O_3 and ZrO_2-XHfO_2 (X=0,10 and 30m/o) were made by mixing appropriate amounts of the single oxides then annealing at 1350°C for 24 hours to form solid solutions. These solid solutions were attrition milled separately for 4 and 8 hours respectively.

The resulting powders were mixed (wet ball mill), dried, isostatically pressed (170MPa) and sintered at 1550°C for 2 hours in an induction furnace with a graphite susceptor and an argon atmosphere. High densities (>98%T.D.) were achieved by maintaining a low oxygen partial pressure atmosphere during sintering. Using this procedure, twelve different compositions, as shown in Table 1, were prepared.

The indentation technique (1) was used to measure fracture toughness. Tetragonal phase content measurements were made on as-sintered and as-ground surfaces. The tetragonal phase fraction which was retained was calculated by using the method proposed by Porter and Heuer (2).

One composition (Al_2O_3-5m/oCr_2O_3 + 10v/o(ZrO_2-10m/o HfO_2)) was aged in air at 990°C and 1200°C for 1 to 308 hours.

RESULTS AND DISCUSSION

Microstructure

A typical photomicrograph of a sample containing 5m/o Cr_2O_3 in Al_2O_3(matrix) and a pure ZrO_2 dispersed phase (10v/o) is shown in Figure 1. The mean dispersed phase grain size is approximately 1um and the mean matrix grain size is approximately 2-3um with a bimodal grain size distribution. The density is >98% of theoretical density. Preliminary microstructural examination indicates that the matrix and dispersed phase grain size is independent of composition and volume fraction of the dispersed phase. The

dispersed phase occurs almost exclusively intergranularly.

Fracture Toughness

The variation of fracture toughness with the volume fraction and composition of the dispersed phase is shown in Figure 2. For both 0 and 10m/o HfO_2 compositions the peak in this curve occurs at 10 ±2v/o and the measured values exceed those of Al_2O_3-5m/oCr_2O_3 solid solutions without ZrO_2 additives. The fracture toughness of the 10m/o HfO_2 samples is greater than that of the 0m/o HfO_2 samples in most cases. The maximum K_{IC} value for the 30m/o HfO_2 samples occurs at ≃5v/o. However, the fracture toughness decreases only slightly for 10 and 12.5v/o dispersed phase and a well defined peak is not observed. For all volume fractions except 5v/o, the fracture toughness of the 30m/o samples was below that for the 0 and 10m/o samples. These results show trends similar to reported results on testing of zirconia toughened alumina in which the peak position and height of the maximum depends on the particle size and composition of the dispersed phase (3,7). For a constant composition and processing schedule, the peak in the K_{IC} versus volume fraction curve has been shown to shift to lower volume fractions and lower K_{IC} values as the starting particle size is increased (4-6). However, the absolute particle size is not nearly as important as the ratio of the particle size to the critical particle size. Optimum toughening will depend on the mechanisms responsible for toughening and on the

ratio of the mean particle size, d, to the critical particle size for spontaneous transformation on cooling, d_c. If the ratio d/d_c is small there should be little toughness enhancement because the very small tetragonal particles are too small to transform to the monoclinic symmetry even in the very high stress field of the crack tip; no transformation toughening occurs. As this ratio increases, the peak should shift to higher K_{IC} values and lower volume fraction values as transformation toughening becomes active. This trend will continue until d/d_c is at or near unity at which point any further increases in d/d_c should cause peak shifts to lower volume fractions and lower K_{IC} values. At very high values of d/d_c the curves should be relatively flat as few tetragonal particles are available for transformation toughening. Microcrack toughening, however, may become active for these materials at very large values of d/d_c.

The peak position of the maximum shifts to higher volume fractions but lower K_{IC} values as Y_2O_3 or CeO_2 is added to zirconia (3,6,7) if the particle size is kept constant. This effect occurs because the critical particle size increases as the amount of Y_2O_3 is added. Thus, the ratio d/d_c, for a constant particle size, decreases with increasing amounts of Y_2O_3. The addition of hafnia to raise the transformation temperature (11,12) causes a shift of the K_{IC} maximum to lower volume fraction values and higher K_{IC} values, provided that the particle size is constant and that

d/d_c does not reach some critical value (at or near unity) at which point the maximum will occur at lower volume fractions and lower K_{IC} values. Although the peaks in Figure 2 for the 0 and 10m/o HfO_2 samples both occur at ≃10v/o, the fracture toughness of the 10m/o samples is greater than that for the 0m/o HfO_2 samples. The fact that the peak occurs at the same volume fraction may be attributed to the relatively large volume fraction increments studied. The fracture toughness curve for the 30m/o HfO_2 samples does not continue this trend. In fact, the fracture toughness of the 30m/o HfO_2 material is considerably lower than that for the samples with lower HfO_2 contents and the observed variation in toughness with volume fraction suggests that no substantial peak in toughness is present. Although it has not been substantiated, it is possible that d/d_c is too large to contribute to transformation toughening.

Tetragonal Phase Measurements

The retained tetragonal phase content data as a function of volume fraction (V_v) and hafnia content after sintering is shown in Figure 3. This data suggests that increasing the hafnia content decreases the retained tetragonal phase content. Assuming that the particle size is constant for a given value of V_v, these results support the hypothesis that hafnia additions to ZrO_2 increase the driving force for transformation and the transformation

temperature, and result in a smaller critical particle size for transformation.

These data also show that the tetragonal phase content decreases with increasing volume fraction dispersed phase. There are three possible reasons for these results. First, the possibility of agglomeration increases as the volume fraction increases. Second, the rate of Ostwald ripening is expected to increase as the volume fraction of dispersed phase increases. Third, the critical particle size may change as a function of the volume fraction of dispersed phase. Claussen (11) has shown that a decrease in tetragonal phase content with increasing volume fraction dispersed phase occurs. Claussen et. al. (5) have shown that the transformation temperature is lowered with decreasing volume fractions of dispersed phase. In addition, Green (10) has shown that the critical particle size decreases with increasing volume fraction dispersed phase. Lange (3), Green (10), and Claussen et. al. (5) have proposed that the reason for the decrease in retained tetragonal phase content with increasing volume fraction dispersed phase is due to the lower modulus of the dispersed phase resulting in a loss of matrix constraint. Excessive agglomeration has not been detected in the microstructures examined and qualitatively the particle size is nearly constant for all samples. The data shown in Figure 3 is consistent with previous work and can probably be attributed to a decrease in the critical particle size with increasing

volume fraction dispersed phase.

Ageing

In order to determine if microstructural or mechanical property changes occurred after extended times at elevated temperatures, Al_2O_3-5m/oCr_2O_3 + 10v/o(ZrO_2-10m/oHfO_2) samples were annealed at 990°C and 1200°C for times up to 308 hours. The results are shown in Figures 4-6. These results show that there is essentially no change in the amount of retained tetragonal phase with ageing time at either temperature. The results of the fracture toughness and hardness testing also show no apparent change with ageing time or temperature (Figure 6). The scatter in the data can probably be attributed to sample inhomogeneity. Qualitative microstructural examination reveals that no microstructural changes occurred in these samples even after extended ageing times.

CONCLUSIONS

1. For the processing conditions studied, the best mechanical properties occurred for the ZrO_2-10m/oHfO_2 compositions.
2. High (30m/o) HfO_2 additions result in low tetragonal fractions and low measured K_{IC} values.
3. Ageing at 990°C and 1200°C for times up to 308 hours resulted in no decrease in tetragonal fraction or measured K_{IC}.

REFERENCES

1. Tien, T.Y., "Transformation Toughened Ceramics - A Potential Material for Light Diesel Engine Application", AMMRC TR 84-46.

2. Porter, K.L., and Heuer, A.H., "Microstructural Development in MgO Partially Stabilized Zirconia (Mg-PSZ)", J. Amer. Cer. Soc., 62, 5-6, 1979, 298-305.

3. Lange, F.F., "Transformation Toughening Part 3 - Experimental Observation in the ZrO_2-Y_2O_3 System", J. Mat. Sci., 17, 1982, 240-46.

4. Claussen, N., "Fracture Toughness of Al_2O_3 with an Unstabilized ZrO_2 Dispersed Phase", J. Amer. Cer. Soc., 59, 1-2, 1976, 49-51.

5. Claussen, N., Steeb, J., and Pabst, W., "Effect of Induced Microcracking on the Fracture Toughness of Ceramics", Cer. Bull., 56, 6, 1977, 559-62.

6. Claussen, N., "Transformation-Toughened Ceramics", Eur. Colloq. on Ceramics in Advanced Energy Technologies, Sept. 1982.

7. Lange, F.F., "Transformation Toughening Part 4 - Fabrication, Fracture Toughness, and Strength of Al_2O_3-ZrO_2 Composites", J. Mat. Sci., 17, 1982, 247-54.

8. Ruh, R., Garett, H.J., Domagala, R.F., and Tallan, N.M., "The System Zirconia-Hafnia", J. Amer. Cer. Soc., 51, 1, 1968, 23-27.

9. Claussen, N., Sigulinski, F., and Ruhle, M., "Phase Transformation of Solid Solutions of ZrO_2 and HfO_2 in an Al_2O_3 Matrix", Advances in Ceramics, Vol. 3, 1891, 164-167.

10. Green, D.J., "Critical Microstructures for Microcracking in Al_2O_3-ZrO_2 Composites", J. Amer. Cer. Soc., 65, 12, 1982, 610-14.

11. Claussen, N., "Stress-Induced Transformation of Tetragonal ZrO_2 Particles in Ceramic Matrices", J. Amer. Cer. Soc., Discussion and Notes, 61, 1-2, 1978, 85-86.

TABLE 1

Matrix Composition	Dispersed Phase Composition	Volume Fraction (v/o)
Al_2O_3-5m/oCr_2O_3	ZrO_2	5
"	"	7.5
"	"	10
"	"	12.5
Al_2O_3-5m/oCr_2O_3	ZrO_2-10m/oHfO_2	5
"	"	7.5
"	"	10
"	"	12.5
Al_2O_3-5m/oCr_2O_3	ZrO_2-30m/oHfO_2	5
"	"	7.5
"	"	10
"	"	12.5

FIGURE 1 MICROSTRUCTURE OF Al_2O_3-5m/oCr_2O_3/ZrO_2(10v/o) COMPOSITE SINTERED FOR 2 HOURS AT 1550°C.

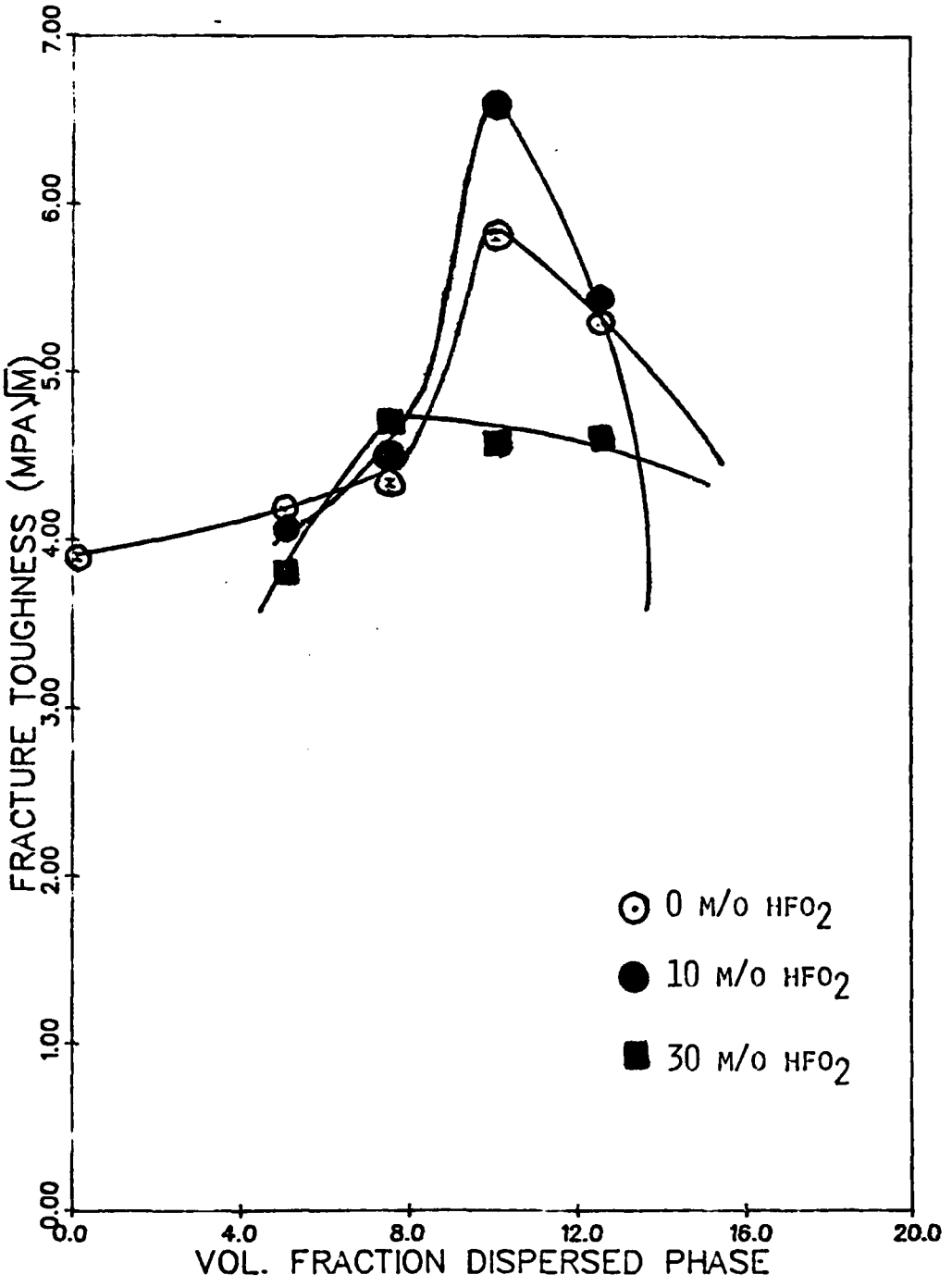

FIGURE 2 FRACTURE TOUGHNESS VERSUS VOLUME FRACTION DISPERSED PHASE.

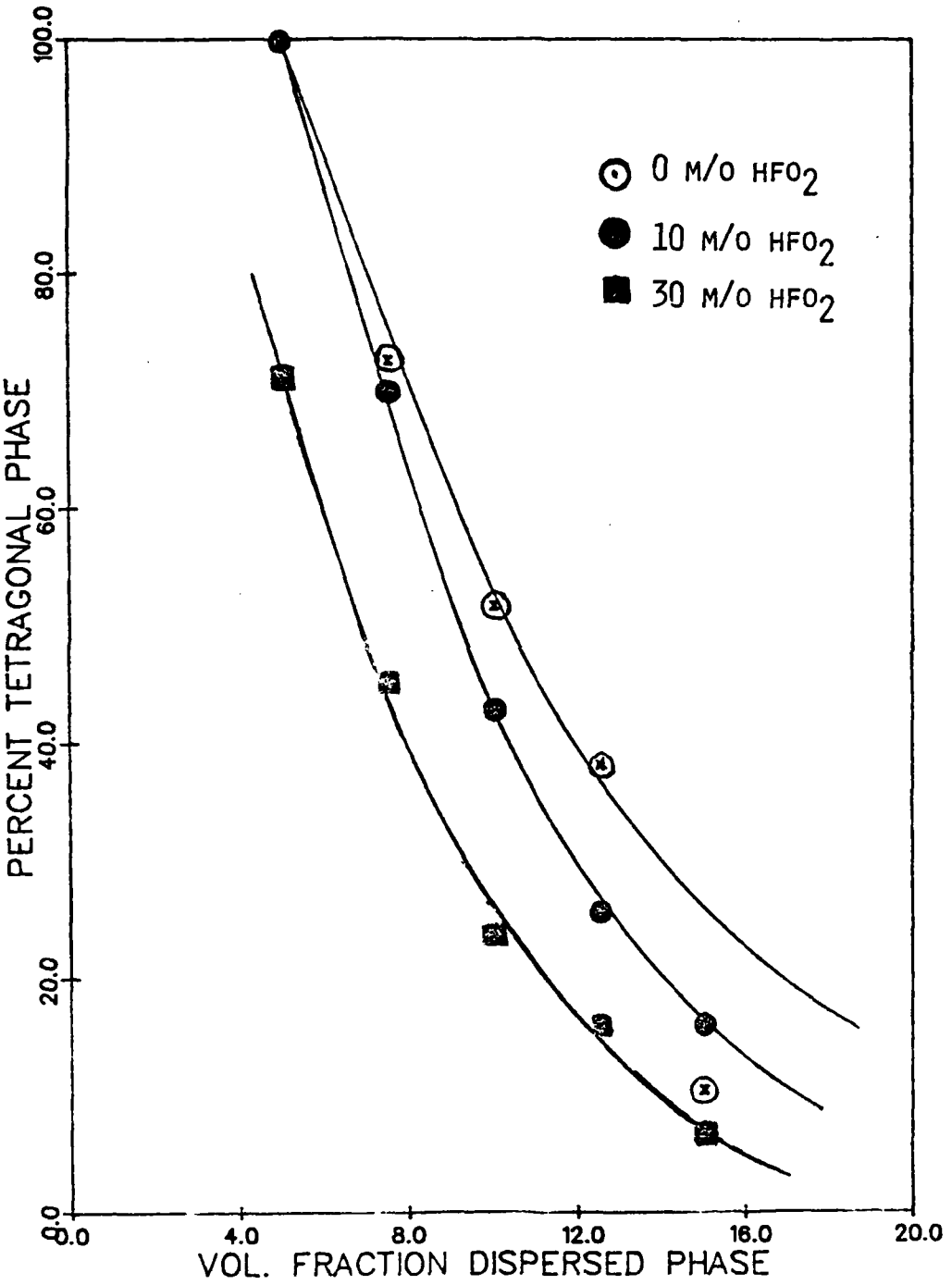

FIGURE 3. PERCENT TETRAGONAL PHASE VERSUS VOLUME FRACTION DISPERSED PHASE.

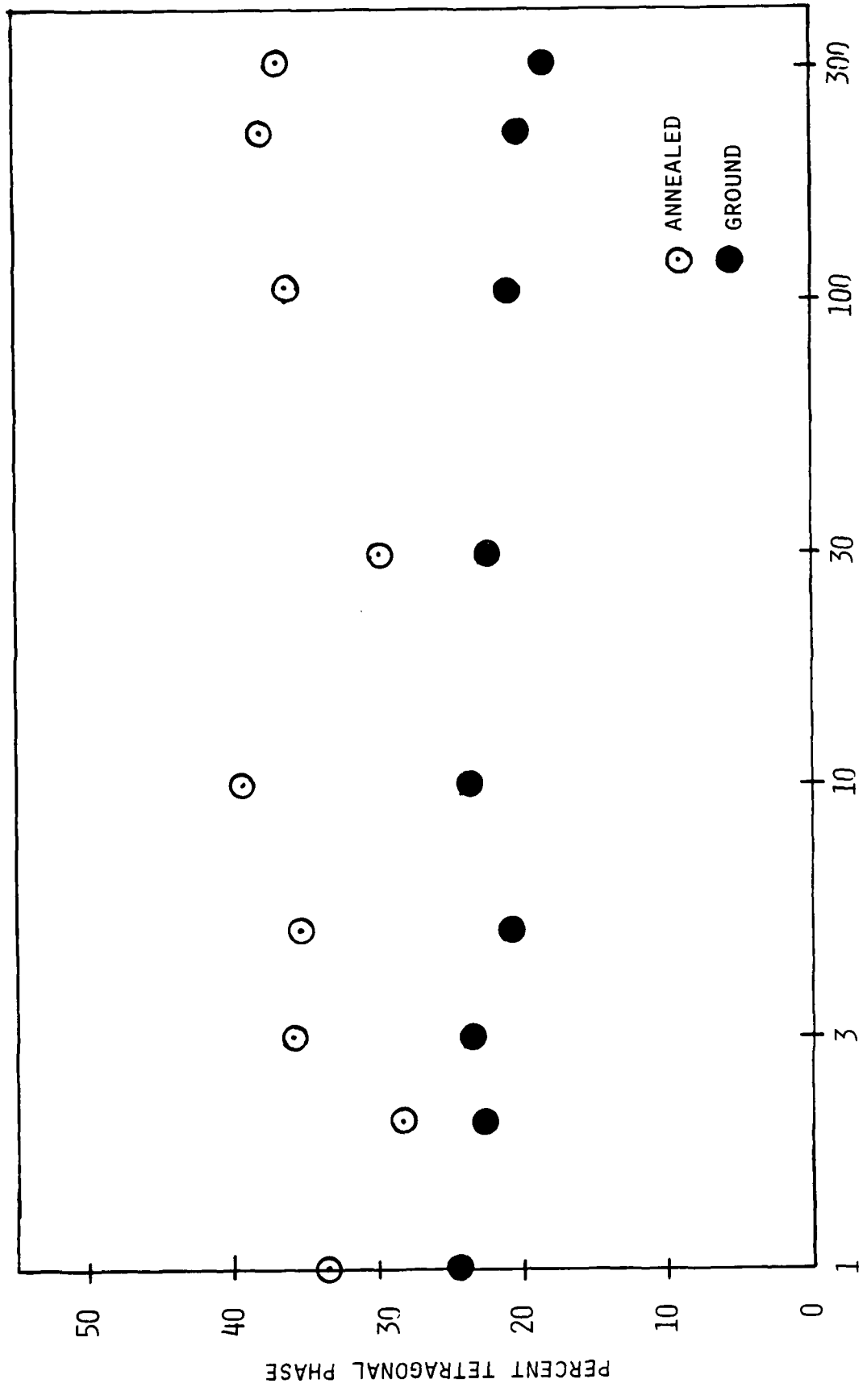

FIGURE 4. PERCENT TETRAGONAL PHASE VERSUS TIME AT 990°C.

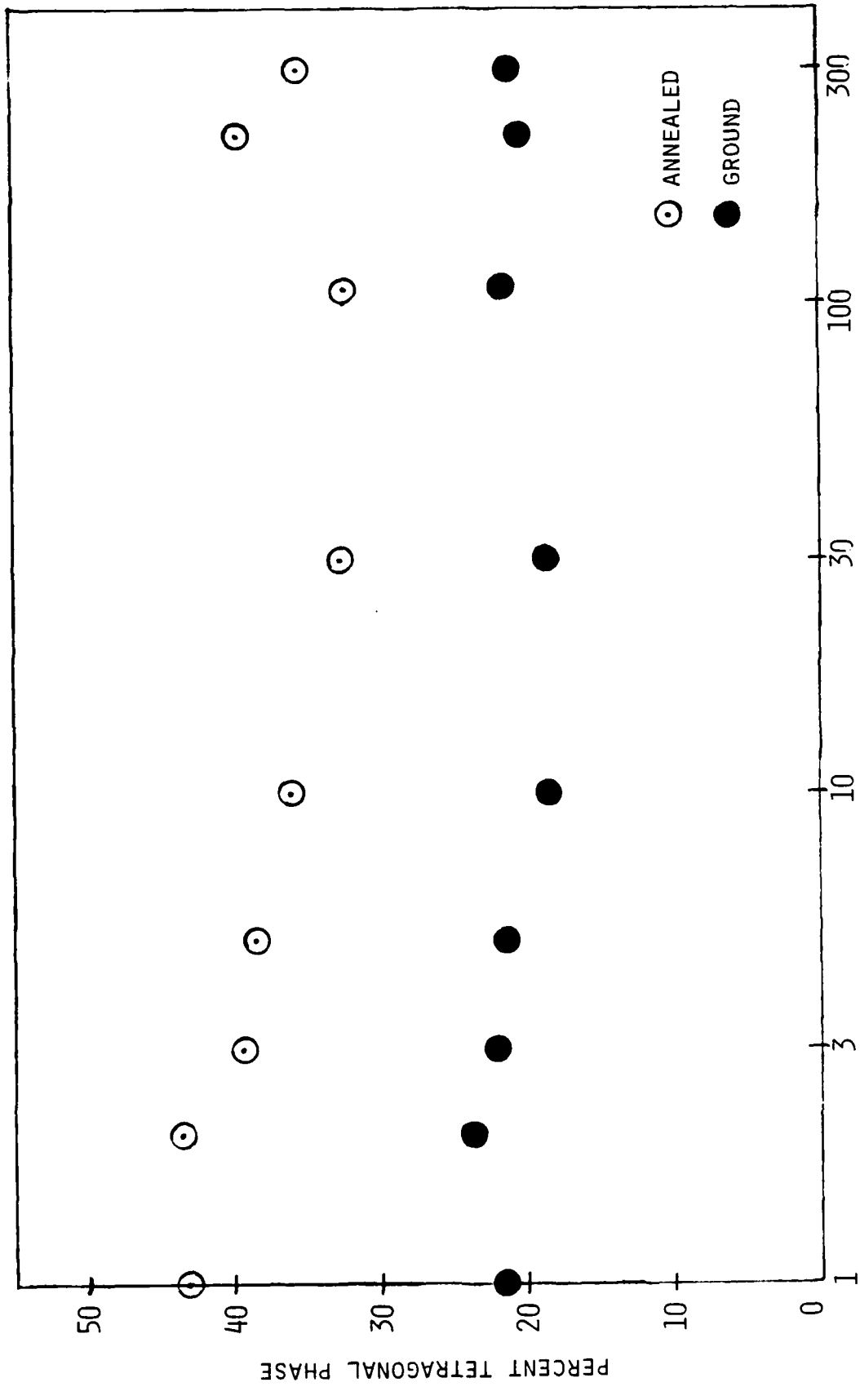

FIGURE 5. PERCENT TETRAGONAL PHASE VERSUS TIME AT 1200°C.

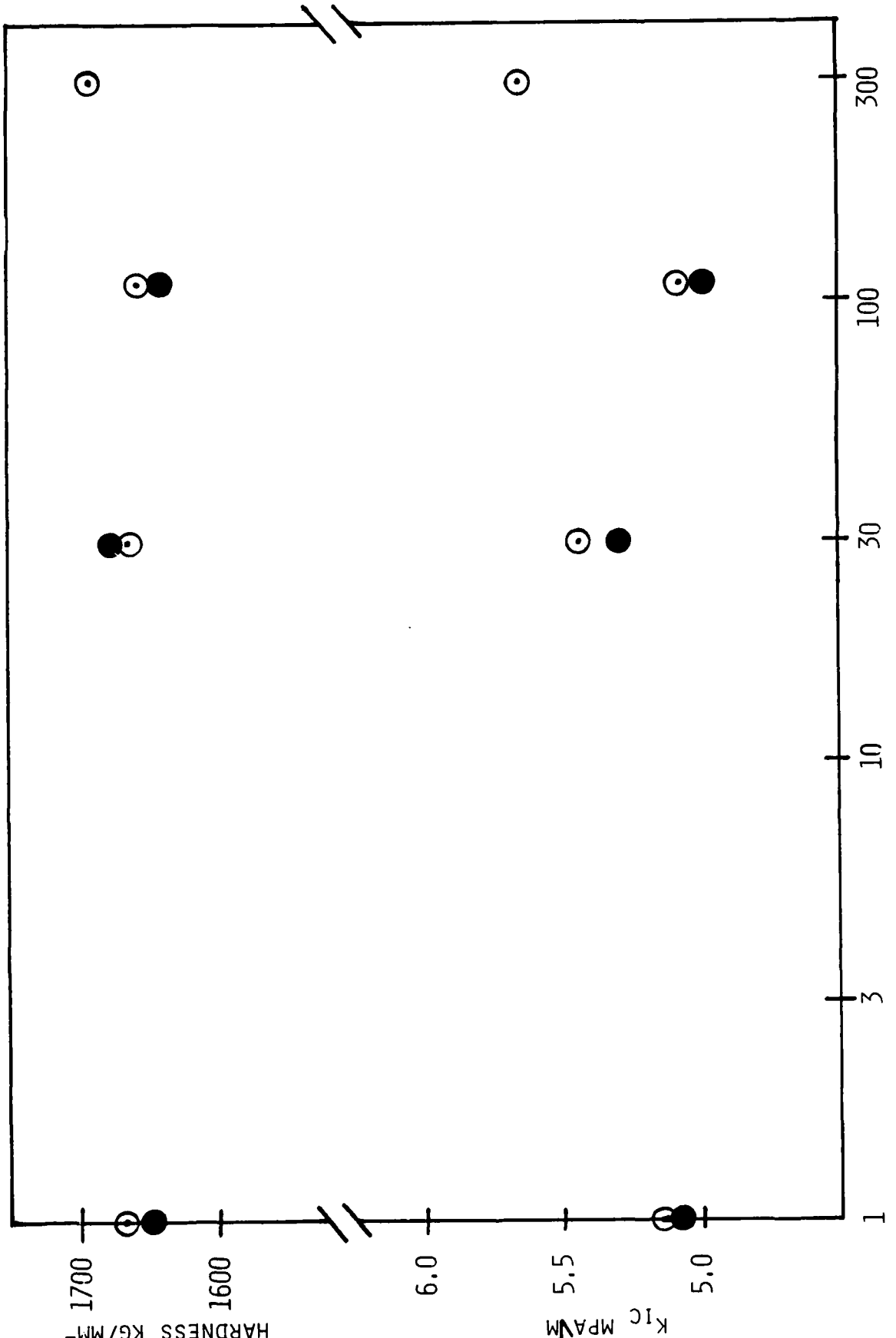

FIGURE 6. HARDNESS AND FRACTURE TOUGHNESS VERSUS TIME AT 990°C (⊙) AND 1200°C (●).

Appendix B

The Therma Diffusivity and Conductivity of Transformation-Toughened Solid-Solutions of Alumina and Chromia

by

R. Syed,* D. P. H. Hasselman,* T.-Y. Tien,+

*Department of Materials Engineering
Virginia Polytechnic Institute and State University
Blacksburg, Virginia 24061 USA

+Materials and Metallurgical Engineering
The University of Michigan
Ann Arbor, Michigan 48109 USA

ABSTRACT

The thermal diffusivity of a series of solid-solutions of alumina and chromia transformation-toughened with a dispersed phase of unstabilized zirconia was measured by means of the laser-flash method from room temperature to 1400°C. It was found, in general, that the thermal diffusivity could be decreased significantly by the combined effects of solid-solution alloying, microcracking and by the presence of the low conductivity dispersed phase of zirconia. The decrease in thermal diffusivity by microcracking was found to be present in the solid-solution with low chromia content which underwent extensive grain growth. The effectiveness of solid-solution formation and microcracking on thermal diffusivity was found to be greatest at the lower and intermediate ranges of temperature. The decrease in the thermal diffusivity due to the zirconia inclusions was found to be effective over the total temperature range. A numerical example is presented for the thermal conductivity calculated from the diffusivity multiplied by the volumetric heat capacity.

1. Introduction

The increasing trend in many fields of engineering such as energy-conversion, chemical processing and aerospace, towards ever increasing operating temperatures places complex demands on the development and selection of materials to meet design requirements and long-term satisfactory performance. In general, candidate materials for functions which involve high temperature should exhibit melting points well in excess of the use temperature, as well as high chemical and structural stability. For specific design situations, the magnitude of the thermo-physical properties also can play a vital role in assuring prescribed performance criteria. For instance, materials for heat-exchangers should exhibit values for thermal conductivity as high as possible. In contrast, for many other designs, the choice of the optimum material is based on its thermal insulating ability which requires values for thermal conductivity which are as low as possible.

Structures and components which operate at high temperatures inevitably are subjected to high steady-state or transient heat fluxes. The resulting spatially non-uniform temperature distributions can lead to thermal stresses of high magnitude. Because of their nature of atomic bonding and more complex crystal structures candidate materials for high temperature service tend to be highly brittle. Because of such brittleness, failure under the influence of thermal stresses can be highly catastrophic, rendering the structure or component totally unsuitable for continued satisfactory service [1]. For this reason, in the design and selection of materials considerable emphasis must be placed on avoiding failure by thermal stresses. It has been established in general, that materials with high resistance to thermal stress failure should exhibit high values for the tensile fracture stress and thermal conductivity

in combination with low values for the coefficient of thermal expansion and Young's modulus of elasticity [2,3]. High fracture toughness also is desirable as it will assure a high tensile failure stress for a material with given crack size; more important is that a high fracture toughness also assures rapid crack arrest following the initiation of thermal crack propagation [1]. This latter criterion is critical for those design situations for which the thermal stresses are of such magnitude that even in the optimum material, the initiation of thermal stress failure cannot be avoided.

It is critical to note that materials with high thermal conductivity chosen specifically to avoid thermal stress failure also will conduct a great deal of heat while in service. Such conduction of heat represents no problem for these designs, such as heat-exchangers, for which the material of construction should exhibit high thermal conductivity in order to meet design requirements.

However, the requirement of high thermal conductivity for resistance to thermal stress failure is incompatible with the requirement of low conductivity for those materials which serve as thermal insulators in those designs for which heat losses must be kept to a minimum. Clearly, for the latter situation design trade-offs need to be made. Alternatively, new materials need to be developed, which exhibit improved thermal insulating ability in combination with enhanced resistance to thermal stress failure. One way this can be achieved is by the inducement of extensive microcrack formation, which lowers thermal conductivity significantly [4], and simultaneously transforms the highly unstable mode of thermal crack propagation to the more desirable stable mode which leads to rapid crack arrest [1]. Unfortunately, spontaneous microcracking leads to a significant decrease in the tensile fracture stress and

possible fracture toughness as well. Clearly, for the development of materials with low thermal conductivity and high fracture toughness an alternative approach must be sought.

One such alternative is to take advantage of a number of independent effects. Significant decreases in thermal conductivity can be achieved by two effects, namely solid-solution alloying [5,6] and the inclusion of second-phase dispersions with a thermal conductivity lower than the matrix material [7,8]. Fracture toughness can be increased significantly by the effect of transformation-toughening, specifically by the addition of a dispersed phase of unstabilized zirconia [9,10]. Such transformation-toughening has been shown experimentally to significantly increase thermal stress resistance as well [11]. Zirconium oxide has a value of thermal conductivity substantially lower than the corresponding value for most structural materials for high temperature applications. For this reason, the presence of a dispersed phase of unstabilized zirconia simultaneously leads to an increase in fracture toughness and thermal stress resistance coupled with a decrease in thermal conductivity. Microcrack formation in the matrix which can be associated with the zirconia dispersed phase can enhance thermal stress resistance and lower the thermal conductivity further. Finally, even lower values of the thermal conductivity can be obtained by choosing a matrix phase which is a solid-solution rather than a high-purity single phase material.

A newly developed material in which the above effects have been combined to achieve the desirable combination of increased fracture toughness and decreased thermal conductivity consists of zirconia-transformation-toughened solid-solution of alumina and chromia. The characterization of

the thermal diffusivity/conductivity of this system is the subject of this study. Mechanical property and other data had been reported by one of the authors (12).

2. Experimental

2.1 Sample Preparation

Specimens used for the thermal diffusivity measurements were made by hot pressing of co-precipitated powder mixtures at 1500°C for 30 minutes under a pressure of 30 MPa. Full densities were obtained for all of the specimens prepared. A carbon resistance furnace and BN coated graphite dies were used for hot pressing these samples.

One half normal solutions containing the metal ions were prepared by dissolving the soluble salts, $Al(NO_3)_3 \cdot 9H_2O$, $Cr(NO_3)_3 \cdot 9H_2O$, $ZrOCl_2 \cdot 3H_2O$ and $HfOCl_2.8H_2O$ in water. Appropriate amounts of solutions were mixed and were added slowly to a NH_4OH solution while stirring. A pH value of 8 of the mixed solutions was maintained during precipitation. The mixtures were kept at 70°C for 30 minutes while stirring. The precipitates were then filtered, washed with dilute amonia solution, and dried at 110°C for 24 hours. The dried precipitates were calcined at 500°C for 2 hours and ground for 10 hours in a ball mill. The calcined powders were amorphous to X-rays.

Figures 1a and 1b show scanning electron micrographs of samples of alumina with 0 and 50 mole % Cr_2O_3 and 15 vol. % ZrO_2. The difference in grain size of the matrix is immediately evident. Because the processing conditions for all samples were the same, it appears that the presence of the chromia acts as a grain-growth inhibitor. Examination of the other samples showed that the grain size decreased monotonically with increasing content of chromia.

2.2 Measurement of thermal diffusivity

The flash method (13) was used for the measurement of the thermal diffusivity, using a glass-Nd laser as the source. The method basically consists of subjecting one face of a specimen in the form of a thin plate to a single laser flash, and monitoring the transient temperature response of the opposite face. The specimens for this study, approx. 8x8 mm square by approx. 2 mm thick, were cut from the larger blocks with the aid of a slow-speed high-precision diamond saw. The surface of the specimens was coated with carbon to assure complete absorption of the energy of the laser flash. For measurements at elevated temperatures the specimens were placed in a suitable holder located in the center of a carbon resistance furnace with nitrogen atmosphere. The transient temperature of the opposite face of the specimen was monitored with a liquid N_2 cooled InSb infra-red detector from ambient temperatures ranging from 25 to about 600°C and with a silicon-photodiode above these temperatures. The total length of time of the measurement of the thermal diffusivity as a function of temperature, including data acquisition during cooling, took approximately six hours.

3. Results and discussion

Fig. 2 shows the data for the thermal diffusivity at room temperature for the alumina-chromia solid-solutions with and without the zirconia dispersed phase as a function of chromia content. For the samples without zirconia the thermal diffusivity exhibits a monotonic decrease with increasing chromia content, with a relative difference of a factor $\simeq 4$ over the total range of chromia content. In general, such a significant decrease

in thermal diffusivity is in qualitative agreement with corresponding data for the thermal conductivity and diffusivity for alumina-chromia solid-solutions reported by others [5,6].

The solid-solution series with zirconia dispersions shows a completely different behavior with the peak value of the thermal diffusivity occurring at an intermediate value of chromia contact. The data for the samples with 20 mole % chromia or higher fall below but are parallel to the data for the samples without zirconia. These differences are thought to be due primarily to the effect of the zirconia particles on the thermal diffusivity. Because zirconia has a thermal diffusivity and conductivity [14,15,16] well below the values for the solid-solution matrix, the zirconia inclusions should result in a decrease in the thermal diffusivity as expected from composite theory [7,8].

The solid-solution samples with zirconia inclusions with less than 20% chromia appear to exhibit an anomalous behavior compared to the solid-solution samples without zirconia inclusions. This apparent anomaly is thought to be related to the extensive grain growth during sintering of the samples with low chromia content. Specifically, it is suggested that this effect is due to the formation of microcracks which occurs more readily in coarse-grained rather than fine-grained materials [17-20]. Because microcracks form preferentially at grain boundaries, they are not readily evident in the SEM-fractographs shown in Fig. 1. However, that the anomoulous behavior is due to microcrack formation can be established by indirect evidence. If no other effects were present it is reasonable to anticipate that the data for the thermal diffusivity of the specimens with 0 and 10 mole % chromia

with zirconia would lie on a curve obtained by extrapolation of the data for the specimens with more than 20 mole % chromia which lies parallel to the curve for the solid-solution specimens without zirconia. The actual experimental value for the samples with 0 and 10 mole % chromia fall below this extrapolated curve by a factor of about three. This latter value agrees with the observed factor of three decrease in the thermal diffusivity of coarse-grained fully microcracked polycrystalline aggregates [21, 22]. The experimental data for the temperature dependence of the thermal diffusivity for the specimens with low chromia content to be presented later also indirectly confirm the presence of microcracks.

For the present samples, microcrack formation can be attributed to two possible effects, namely the mismatch in the coefficients of thermal expansion of the zirconia and the alumina-chromia solid-solution or due to the increase in volume of the zirconia particles as the result of the tetragonal-to-monoclinic phase transformation. X-ray analysis of the samples with the anomously low thermal diffusivity showed the relative amounts of the tetragonal and monoclinic phases not to be significantly different from the samples with 50 mole % chromia which presumable are free of microcracks. This indicates that the thermal expansion mismatch between the zirconia and the alumina-chromia matrix appears to be the primary mechanism of microcrack formation.

Figs. 3a, b, c and d show the experimental data for the temperature dependence of the thermal diffusivity of the solid-solution with 0, 10, 20 and 50 mole % with and without the zirconia dispersed phase. For the specimens with 20 and 50 mole % chromia, at least qualitatively, the temperature dependence is typical for dielectric materials with phonon transport

as the primary mechanism for heat transfer. For the samples with 50% chromia, however, the relative temperature dependence of the thermal diffusivity is less than the corresponding dependence for the samples with 20% chromia. This effect arises because at the higher chromia contents the thermal diffusivity is affected by the temperature independent phonon-solute atom interactions which suppresses the strongly temperature dependent effect of phonon-phonon collisions on thermal diffusivity. In this respect, it is of interest to note that at the highest level of temperature the thermal diffusivity for the samples with 20 and 50 mole % chromia are comparable. This suggests that solid-solution alloying is most effective in lowering the thermal diffusivity at low to intermediate temperatures, rather than at the highest ranges of temperature of this study. In contrast, for the samples with chromia contents of 20 mole % or higher, the zirconia is effective in lowering the thermal diffusivity by about twenty percent over the total temperature range.

The samples with 0 or 10 mole % chromia without zirconia, as shown in Figs. 3a and 3b, exhibit a temperature dependence typical for a dielectric with phonon transport as the primary mechanism for heat conduction. The data for the alumina without chromia and zirconia compare very favorably with the values which can be inferred from the data for the thermal conductivity of pure high-density alumina [5].

The samples with 0 and 10 mole % Cr_2O_3 with the zirconia as shown by the data given in Figs. 3a and 3b, exhibit a temperature dependence which is distinctly different from the corresponding behavior for the other samples. The data obtained during cooling from the higher temperature do not retrace the data obtained during the initial heating phase of the heating-

and-cooling cycle. Both these effects are typical for polycrystalline aggregates [21,22] and composites [23] which undergo extensive microcracking. The suppressed temperature arises from two mutually compensating effects. The thermal diffusivity will decrease with increasing temperature due to the normal phonon processes. This effect, however, is offset by crack-closure and possibly crack-healing on heating the specimen towards the temperature at which it was fabricated, which would lead to an increase in thermal diffusivity.

At the highest levels of temperature crack healing can take place by diffusional or other processes which should lead to an increase in the thermal diffusivity. For this reason, during a heating-and-cooling cycle the data on cooling, at least at those temperatures at which no new microcrack formation will occur, should exceed the values obtained during the heating phase of the cycle, as observed.

It should also be noted that Figs. 3a and 3b indicate that the data obtained on cooling cross over the data on heating, so that on return to room temperature the thermal diffusivity exhibits a permanent decrease. This effect is thought to be the result of the formation of microcracks in addition to those formed during the initial cooling from the manufacturing temperature. Such an effect is expected if microcrack formation at the higher temperatures involves a stage of sub-critical growth from microcrack-precursors such as pores. If so, the microcrack density would be expected to be a function of time or number of cooling cycles. Regardless of the details the data in Figs. 3a and 3b clearly indicate that the thermal diffusivity and possibly other properties of microcracked materials can be a function of thermal history.

The closure and healing of microcracks at the higher temperatures will cause the thermal diffusivity to approach the value corresponding to the crack-free material. For this reason, the mechanism of microcracking for the reduction of the thermal diffusivity and conductivity is expected to be most effective at the lower ranges of temperature over which the cracks exhibit their maximum size and crack-opening displacement.

For estimates of heat losses, necessary for the purposes of optimizing a specific design, data are required for the thermal conductivity expecially for conditions of steady-state heat flow. These can be obtained by multiplication of the experimental data for the thermal diffusivity with the volumetric heat capacity (i.e., the product of the specific heat and density). For purposes of saving space, as a numerical example, the thermal conductivity was calculated for the solid-solution with 80 mole % Al_2O_3 and 20 mole % Cr_2O_3 using the experimental data in Fig. 3c. The values of the volumetric heat capacity were obtained from the measured value of density and literature data [24] for the specific heat of the individual oxides shown in Fig. 4 which were assumed to be appropriate for the materials of this study. The resulting values of the thermal conductivity are presented in Fig. 5. These values show a similar relative temperature dependence as the data for the thermal diffusivity given in 3c. Because of the increase in specific heat with increasing temperature, quantitatively the relative temperature dependence of the thermal conductivity at any temperature differs from the corresponding temperature dependence of the thermal diffusivity. For all compositions, the earlier conclusions about the relative effects of solid-solution alloying, microcracking and the presence of the zirconia dispersed phase on thermal diffusivity also will apply to the effects of these same variables on thermal conductivity.

In this respect, two general recommendations can be made in regard to the desired composition and associated microstructure which for the present composite system will yield minimum values of the thermal conductivity (i.e., opitmum thermal insulating behavior). As shown in Fig. 4, the value for the specific heat (per unit mass) of the chromia is significantly less than the corresponding value for the alumina especially at the higher values of temperature. Even taking into account the differences in density, the volumetric heat capacity of the chromia still is significantly less than the corresponding value for the alumina. For this reason, the lowest value for the thermal conductivity for the present series of compositions, will be obtained at the highest level of chromia content.

A speculation can be made on how to reduce the thermal conductivity of the compositions of this study even further. As indicated by the data shown in Fig. 2, the relative decrease in the thermal diffusivity at room temperature which can be achieved at the higher levels of chromia content is of the order of the relative decrease attainable by microcracking at zero or low values of chromia content. This implies that if microcracking could be induced in the compositions with the higher value of chromia content, values for the thermal diffusivity and corresponding values for the thermal conductivity would have been achieved significantly lower than those observed. At least in principle, this could be achieved by modifications of the processing conditions such that grain-growth is promoted for those compositions with the higher values of chromia content.

In summary, the results of this study have demonstrated that the thermal diffusivity and conductivity of dielectric materials can be reduced significantly by the combined effects of solid-solution alloying, microcrack formation

and by inclusion of a low thermal conductivity dispersed phase. Unstabilized zirconia as such a dispersed phase had the additional advantage that by the mechanism of phase-transformation toughening, the decrease in thermal diffusivity and conductivity is accompanied by an enhanced fracture toughness as well as thermal stress resistance.

Acknowledgments

The measurement of the thermal diffusivity was conducted as part of a program funded by the Office of Naval Research under Contract N00014-78-C-0431. The specimens were prepared with the support provided by Army Materials and Mechanics Research Center under Contract DAAG-84-C-003.

References

1. D.P.H. Hasselman, J. Amer. Ceram. Soc., 52 (1969) 600.

2. W.D. Kingery, J. Amer. Ceram. Soc., 38 (1955) 3.

3. D.P.H. Hasselman, Bull. Amer. Ceram. Soc., 49 (1970) 1933.

4. D.P.H. Hasselman, J. Comp. Mat. 12 (1978) 403.

5. W.D. Kingery, H.K. Bower and D.R. Uhlmann, Introduction to Ceramics, John Wiley (1976).

6. J.E. Matta and D.P.H. Hasselman, J. Amer. Ceram. Soc., 58 (1975) 458.

7. Z. Hashin, J. Comp. Mat. 2 (1968) 284.

8. S.C. Cheng and R.I. Vachon, Int. J. Heat Mass Transfer, 12 (1969) 249.

9. N. Claussen, J. Amer. Ceram. Soc., 59 (1976) 49.

10. A.G. Evans and A.H. Heuer, J. Amer. Ceram. Soc., 63 (1980) 241.

11. N. Claussen and D.P.H. Hasselman pp. 381-395 in Thermal Stresses in Severe Environments, D.P.H. Hasselman and R.A. Heller, Plenum Press (1980)

12. T.K. Brog, J.W. Jones and T.Y. Tien, Proc. 21st ATDCCM, (1983) 207-214.

13. W.J. Parker, R.J. Jenkins, C.P. Butler and G.L. Abbott, J. Appl. Phys., 32 (1961) 1679.

14. W.D. Kingery, J. Papis, M.E. Doty and D.C. Hill, J. Amer. Ceram. Soc., 42 (1959) 393.

15. V.C. Mirkovitch, J. Amer. Ceram. Soc., 48 (1965) 387.

16. R.C. Garvie, J. Mat. Sc., 11 (1976) 1365.

17. R.W. Rice and R.C. Pohanka, J. Amer. Ceram. Soc., 62 (1979) 559.

18. E.D. Case and J.R. Smyth, Mat. Sc. and Eng., 51 (1981) 175.

19. Y. Fu and A.G. Evans, Acta Met., 30 (1982) 1619

20. A.G. Evans and D.R. Clarke, pp. 629-48 in Thermal Stresses in Severe Environments, D.P.H. Hasselman and R.A. Heller, Eds., Plenum Press (1980)

21. H.J. Siebeneck, D.P.H. Hasselman, J.J. Cleveland and R.C. Bradt, J. Amer. Ceram. Soc., 59 (1976) 241.

22. H.J. Siebeneck, D.P.H. Hasselman, J.J. Cleveland and R.C. Bradt, J. Amer. Ceram. Soc., 60 (1977) 336.

23. L.D. Bentsen and D.P.H.Hasselman, in Thermal Conductivity 18, T. Ashworth Ed., Plenum Press (in press).

24. Y.S. Touloukian, R.W. Powell, C.Y. Ho and M.C. Nicolaou, Thermophysical Properties of Matter, TPRC Series, Vol. 5-Specific Heat-Nonmetallic Solids, Plenum Press, N.Y., 1973.

Figure 1. Scanning electron fractographs of solid-solution of alumina and chromia with 15 vol. % zirconia with a: 0 and b: 50 mole % chromia.

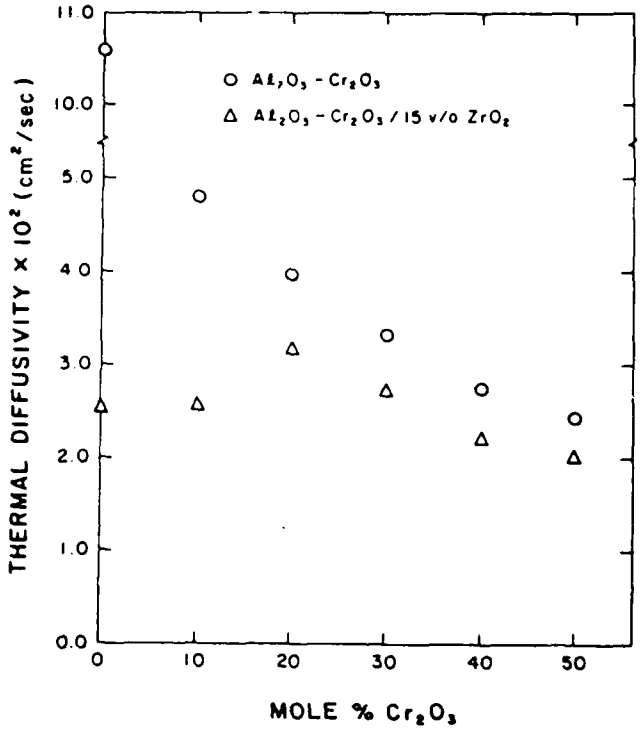

Figure 2. Thermal diffusivity at room temperature of solid-solutions of alumina and chromia with or without a dispersed phase of 15 vol. % zirconia as a function of chromia content.

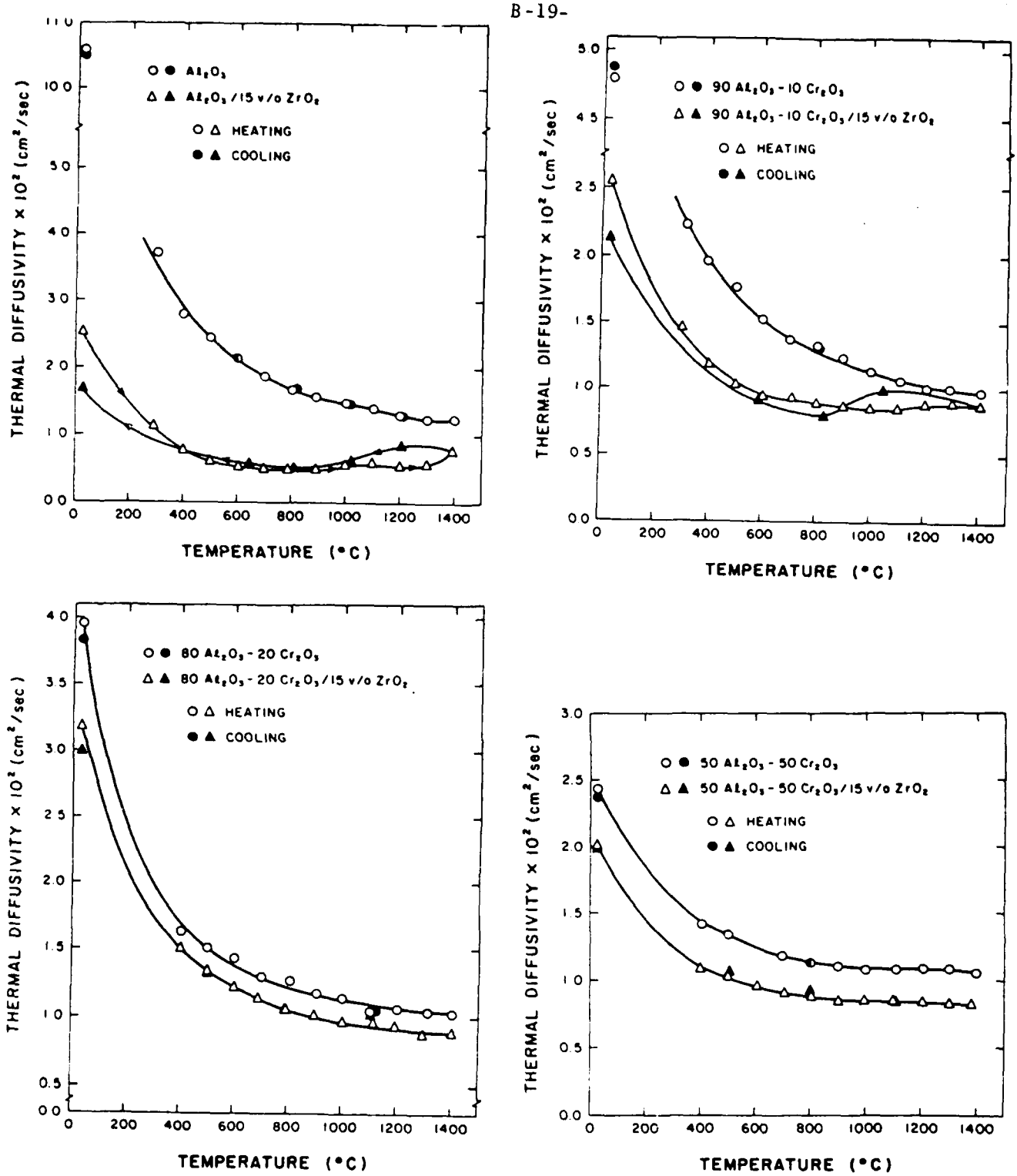

Figure 3. Temperature dependence of the thermal diffusivity of alumina-chromia solutions with or without zirconia inclusions with a:0; b:10; c:20; and d:50 mole % Cr_2O_3.

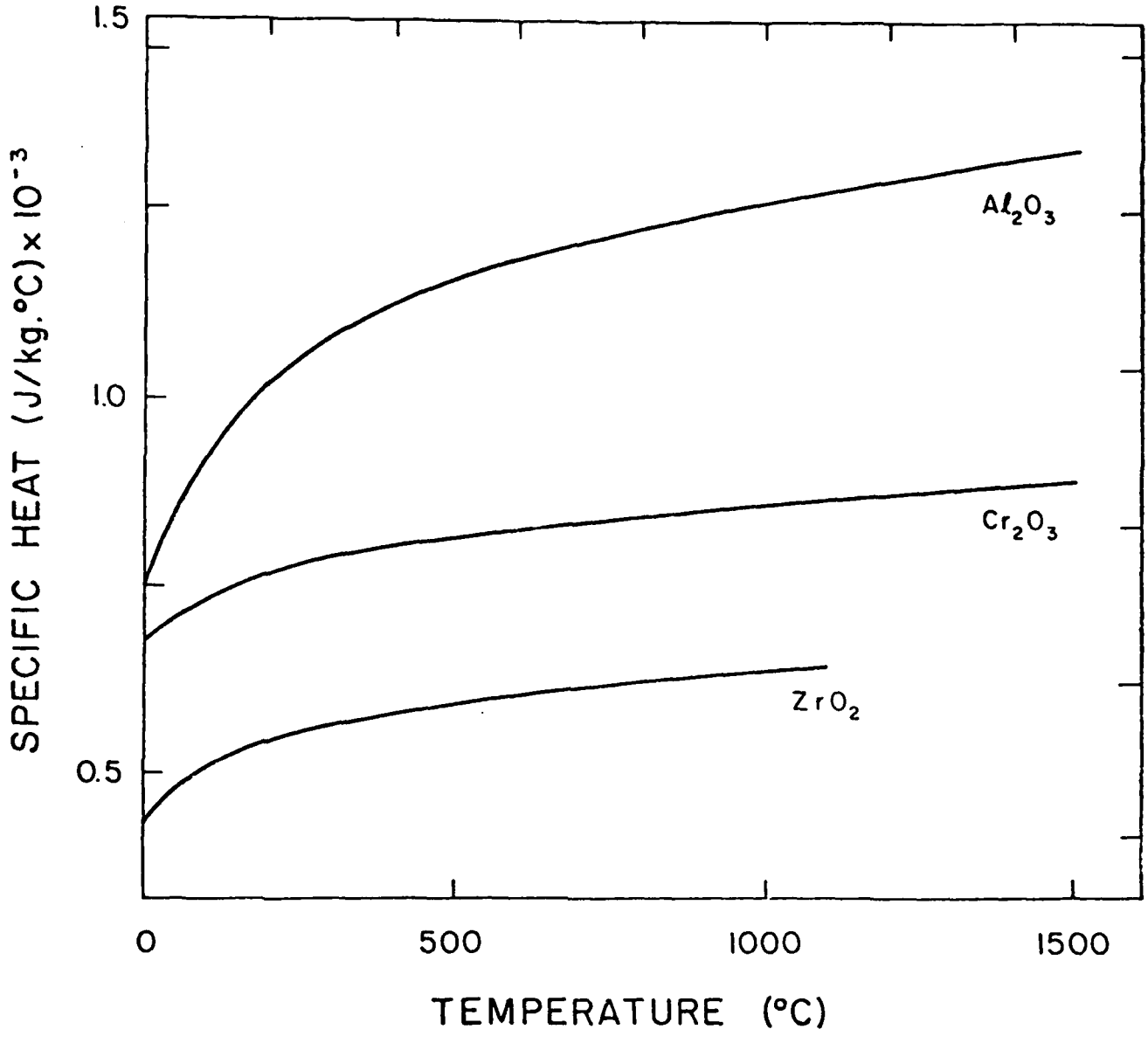

Figure 4. Specific heat of alumina, chromia and zirconia (after Ref. 23).

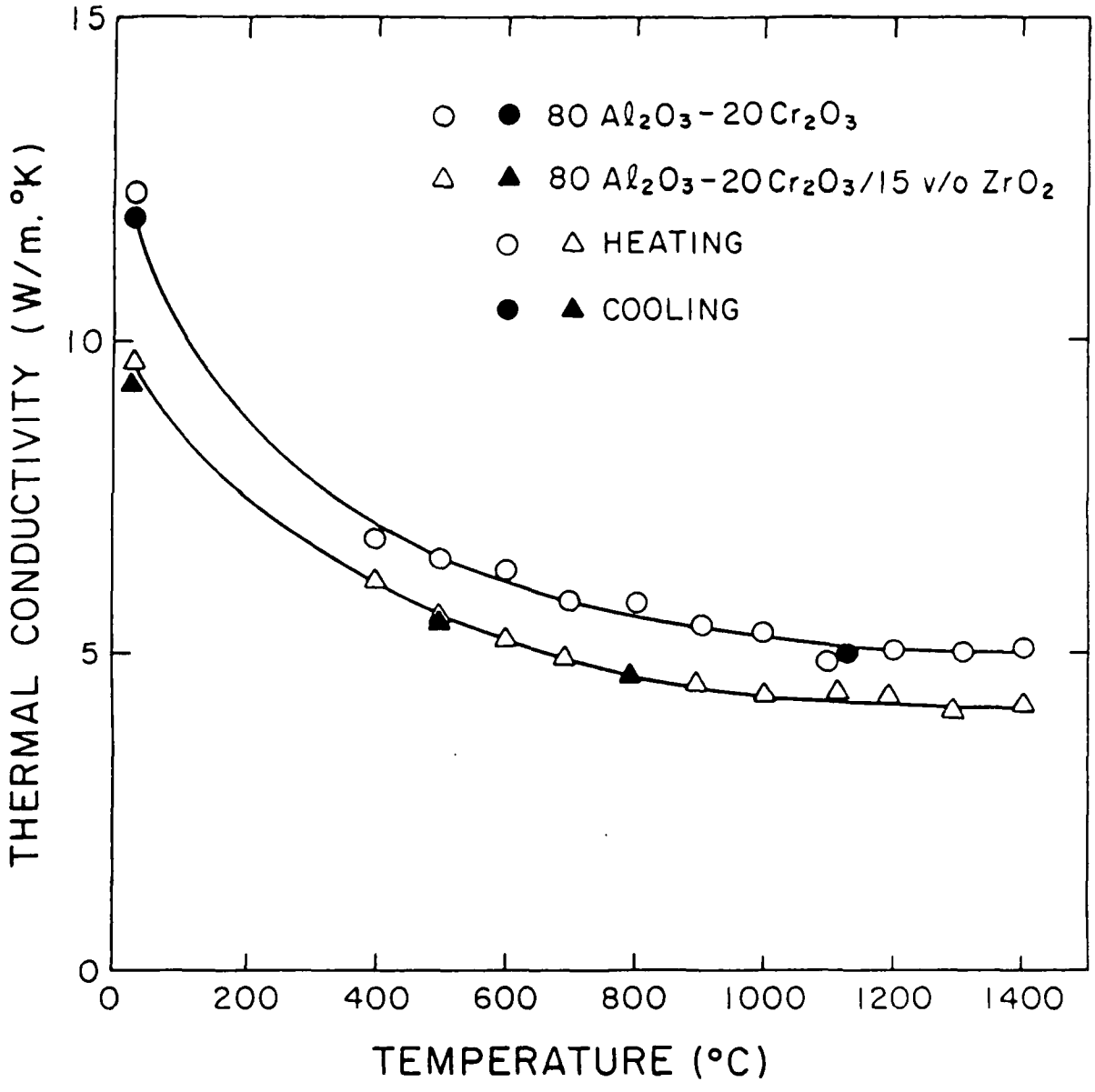

Figure 5. Thermal conductivity of alumina-chromia solid-solution with 20 mole % chromia with and without 15 vol. % zirconia.

Appendix C

Transformation Toughened Mullite with ZrO_2/HfO_2 Solid Solutions

C. K. Yoon and T. Y. Tien

The System Mullite - ZrO_2 - HfO_2:

Compositions studied were mullite containing 15 vol % of $(1-y)ZrO_2:(y)HfO_2$ where y = 0, 0.1 and 0.2.

Aluminum nitrate, zirconium oxychloride, hafnium oxychloride and tetraethoxysilane were used as starting materials. Aqueous solutions of these chemicals were prepared and mixed in appropriate proportions to give the desired compositions. Ethanol was added to the mixtures to prevent separation of the ethoxysilane from the aqueous solution. Mixed solutions were stirred for 30 minutes and then NH_4OH was added drop by drop to the mixtures. When the pH value reached 5.5, stiff gel was formed. The gel was filtered, dried in an oven at 100°C for 24 hours and then calcined at 450°C for one hour. The calcined powders were found to be amphorous to XRD. The powders were then ground in an agate jar mill with agate balls for 10 hours. The ground powders were isostatically pressed at 172 MPa and sintered at 1550, 1600 and 1650°C.

Bulk densities were measured using Archimedes' principle using water as the media. Phase present was determined by XRD and microstructures were examined using SEM on polished and thermal etched surfaces. K_{IC} values for some of the specimens were measured by the microindentation method (1). Five indentations were made at each load level and five load levels were used for each specimen. The amount of tetragonal phase to the amount of monoclinic phase ratio for each specimen was obtained by comparing peak intensity ratio of (111) and $(11\bar{1})$ of the monoclinic phase to the peak intensity of the (111) of the tetragonal phase.

The specimens sintered at 1550°C did not densify (75-82% of the theoretical density). Specimens sintered above 1600°C for a period longer than one hour reached 95% or higher of the theoretical density. Specimens sintered at 1550°C contained $ZrSiO_4$. The zircon phase disappeared at 1600°C.

Grain growth data for the mullite grain in the specimens sintered at 1600 and 1650°C are shown in Fig. 1. Ripening rate of the dispersed particles are given in Fig. 2. Fig. 3 is the same data plotted in a log-log scale. The above data indicated that the presence of HfO_2 and solid solution in the ZrO_2 particles retarded the growth rate.

Microstructures of the mullite with dispersed phase are given in Fig. 4 and 5. The presence of HfO_2 did not seem to affect the microstructure development. Mullite grains in the sintered specimens appeared to be elongated and the dispersed phase located intergranularly. Relative amount of the tetragonal phase of the dispersed ZrO_2 phase are presented in Fig. 6.

Figs. 7 through 9 show the variations of K_{IC} values with particle size of the dispersed phase having different amounts of HfO_2 in solid solution. The K_{IC} value increased with increasing the HfO_2 content when the particle size of the dispersed phase are the same.

Data in Figs. 7, 8 and 9 are compiled and were plotted in Fig. 10. A maximum is shown on the curve. This maximum indicates the critical particle size of the dispersed phase. Unfortunately, the scattering of the data was so large that the effect of the HfO_2 in the dispersed particles is not clear.

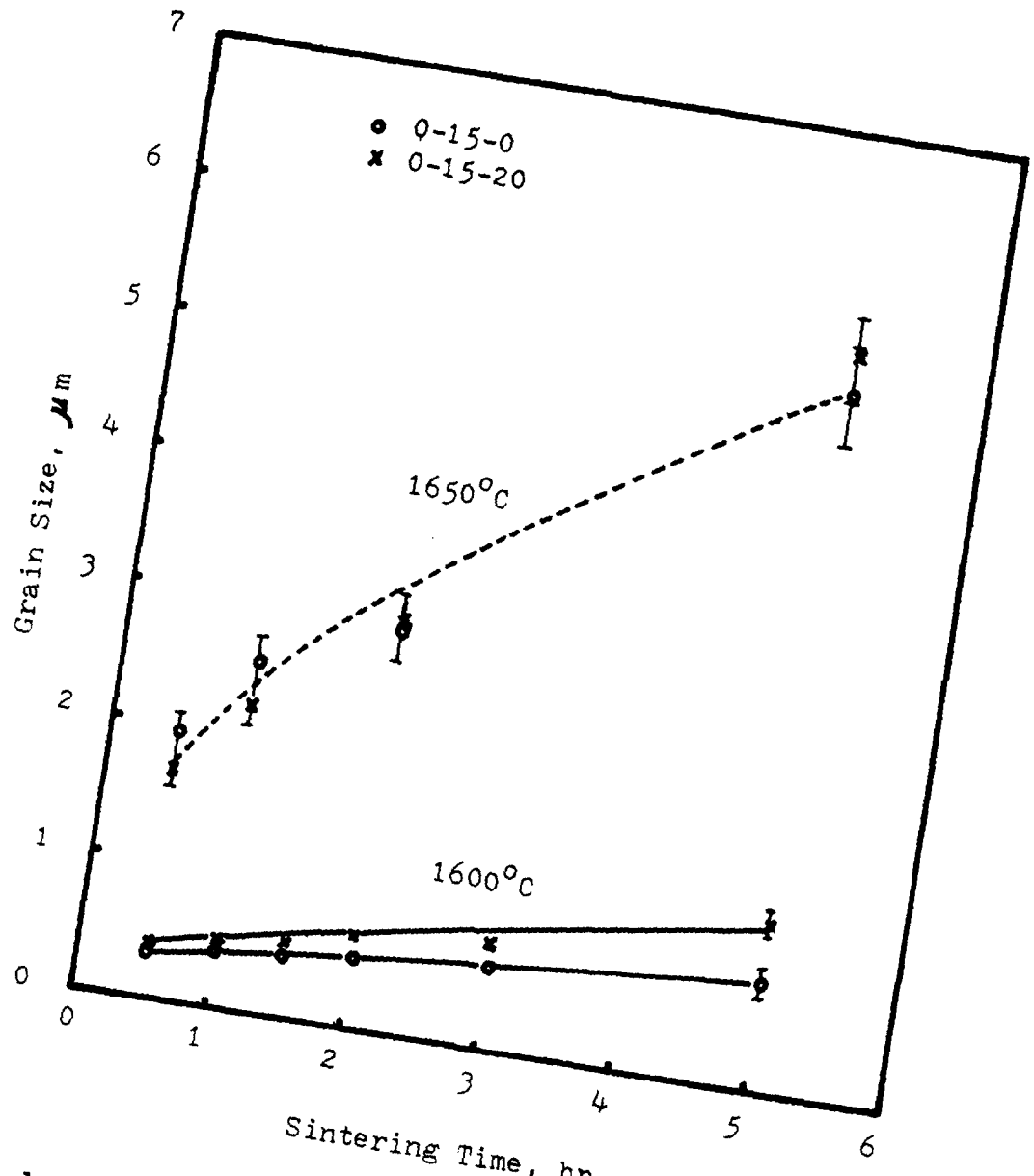

Fig. 1. Grain growth behavior with sintering time at 1600°C and 1650°C.

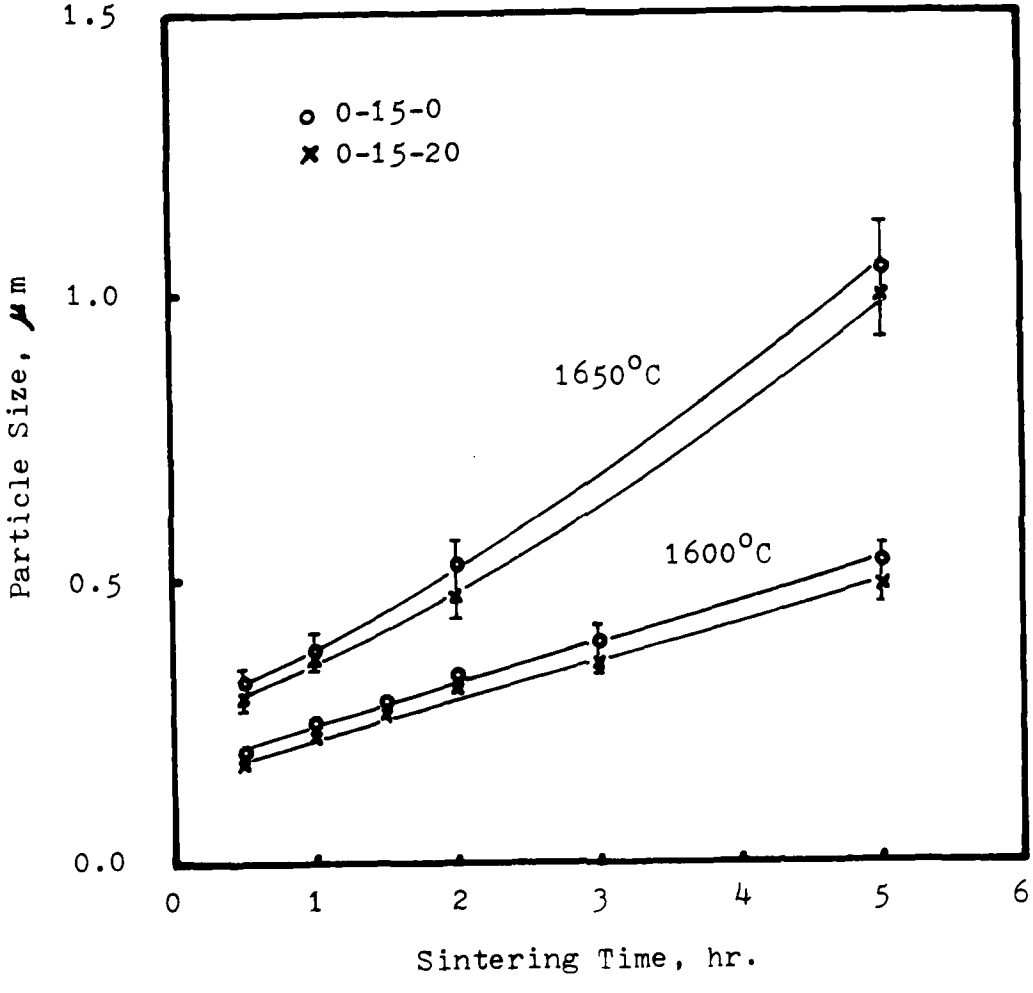

Fig. 2. Variations of particle size with sintering time at 1600°C and 1650°C.

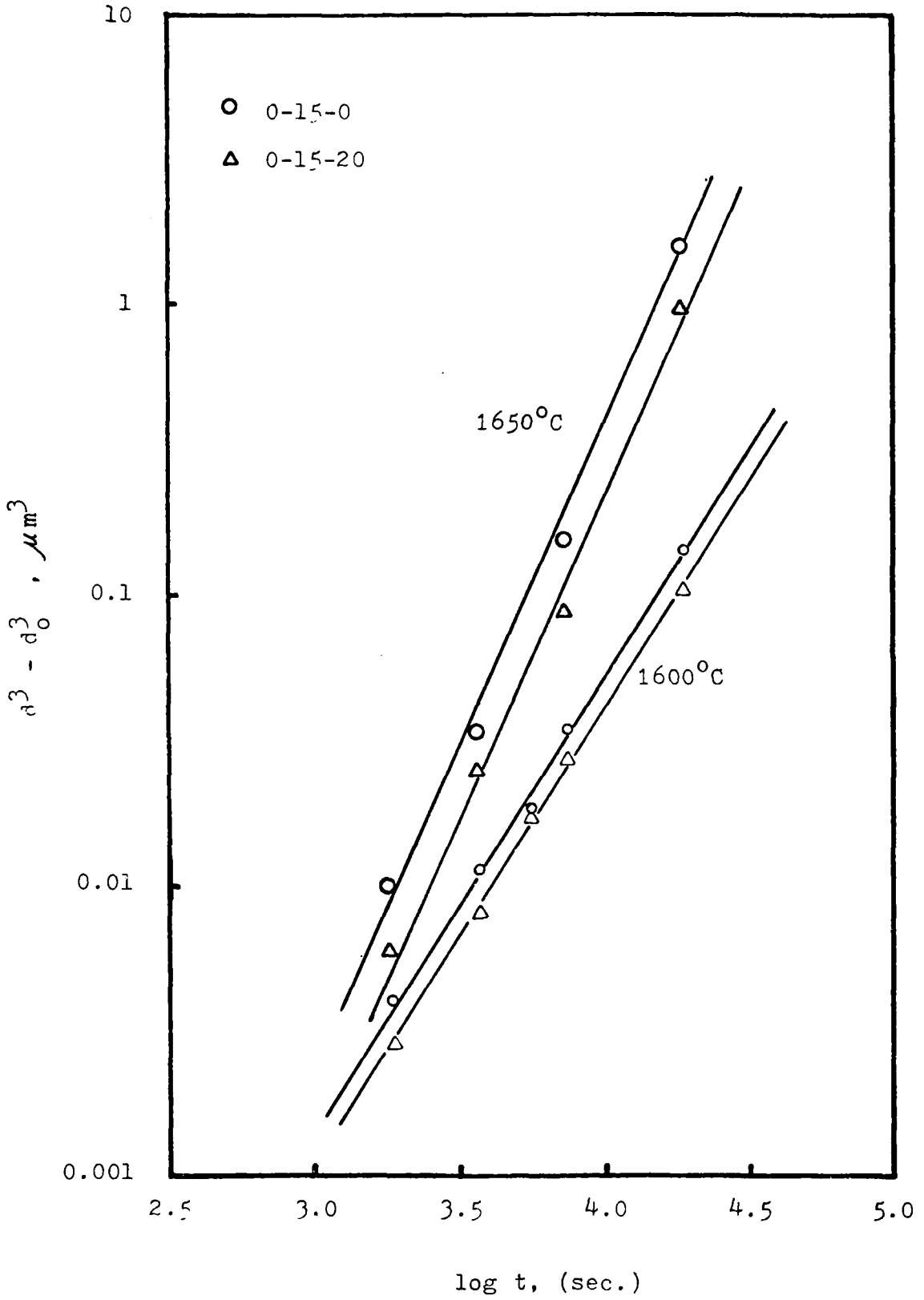

Fig. 3. Log-log plot of isothermal particle growth with sintering time at 1600°C and 1650°C

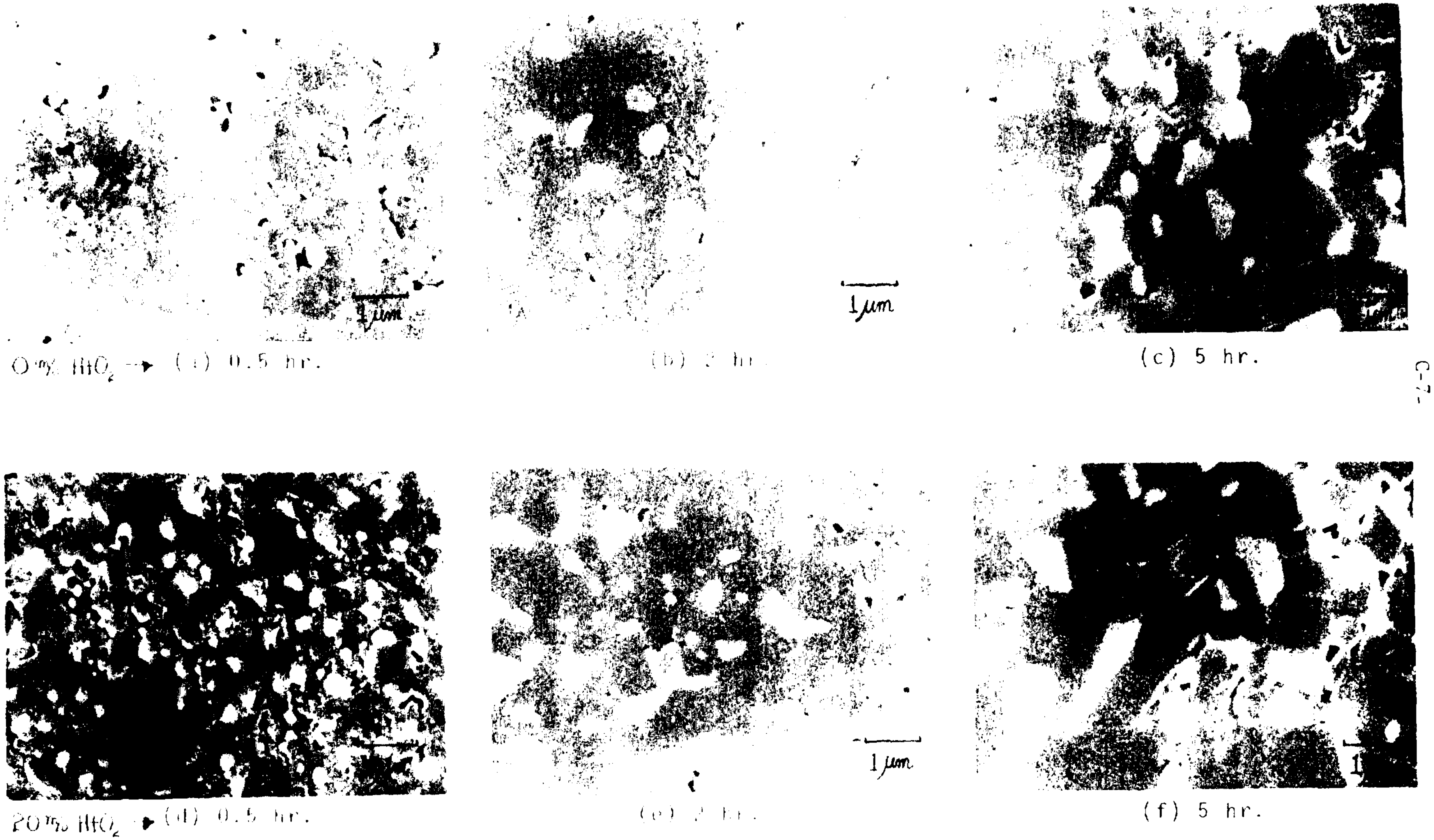

Fig. 4. SEM microstructures of mullite with [illegible] at different HfO_2 content and times at 1600°C. [illegible] thermally etched

0% HfO_2 → (a) 0.5 hr. (b) 2 hr. (c) 5 hr.

20% HfO_2 → (d) 0.5 hr. (e) 2hr. (f) 5 hr.

Fig. 5. SEM microstructures of zirconia with ZrO_2 free Al_2O_3 dispersions at different HfO_2 content and times at 1650°C. Thermally etched.

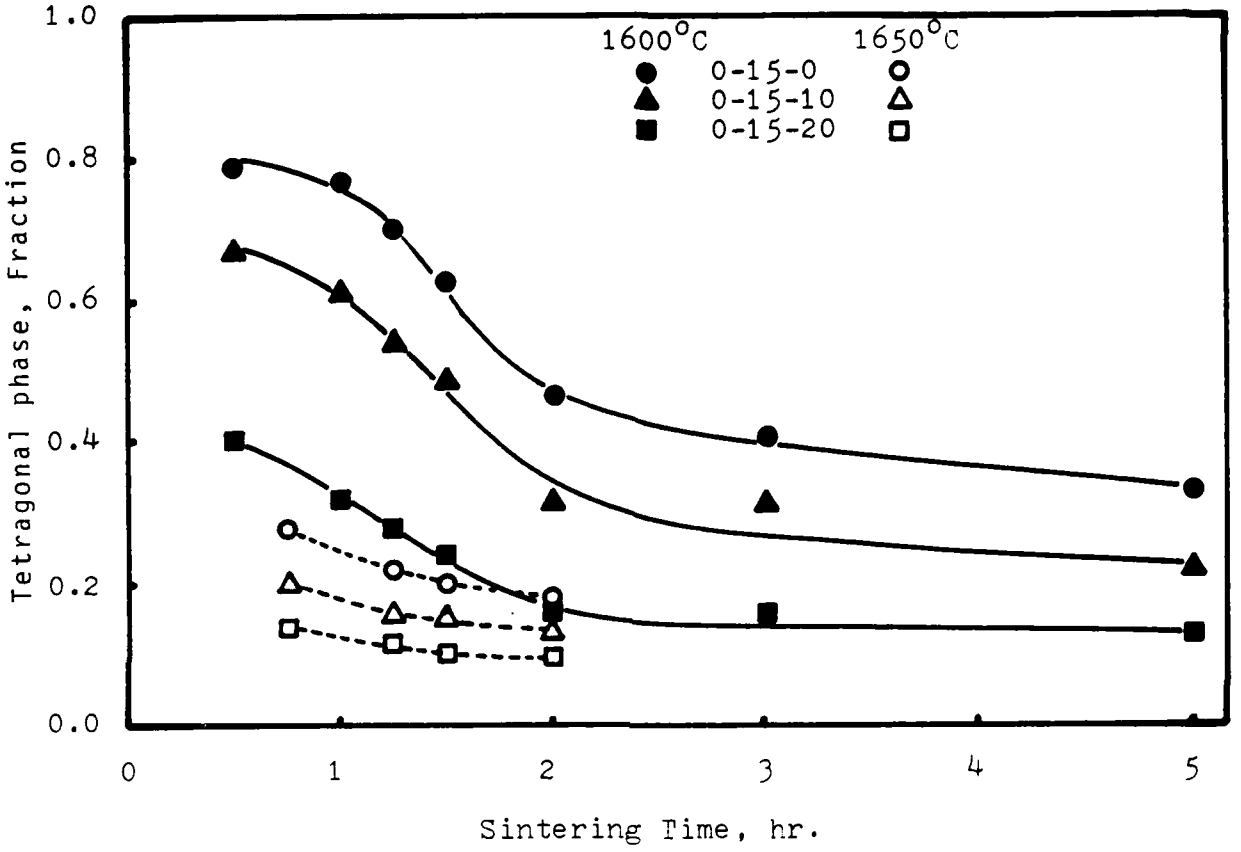

Fig. 6. Variations of amount of tetragonal phase on sintered surface with sintering time in 0, 10, and 20 m/o HfO_2/ZrO_2 particles at 1600°C and 1650°C.

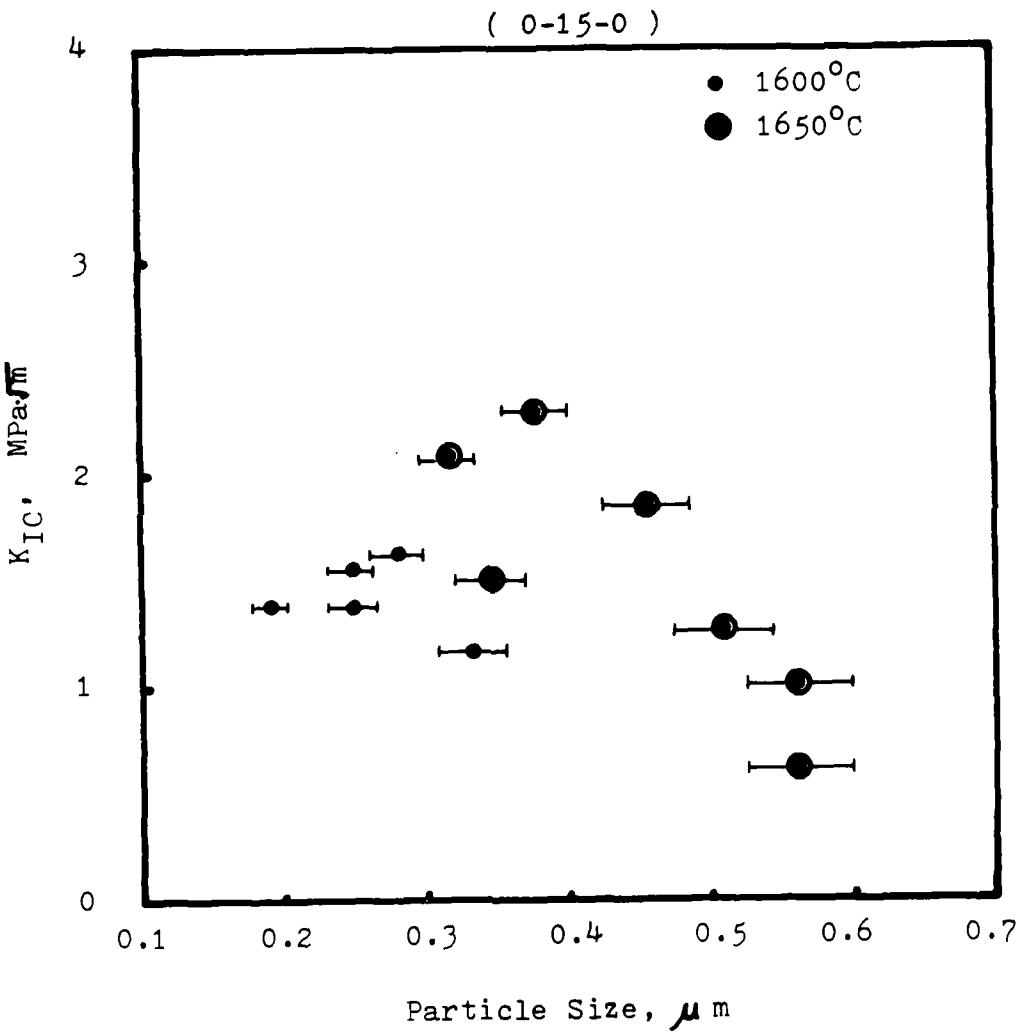

Fig. 7. K_{IC} vs. particle size changes in 0-15-0 specimens

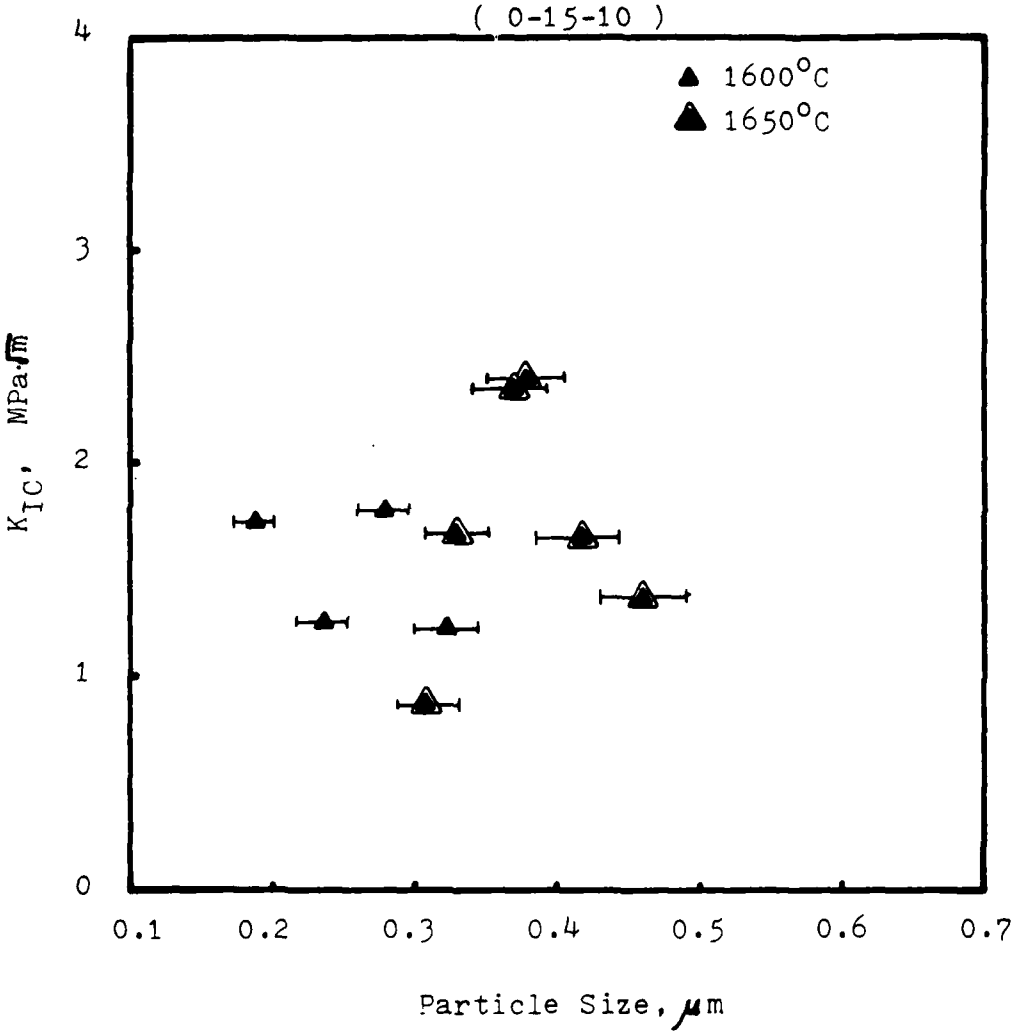

Fig. 8. K_{IC} vs. particle size changes in 0-15-10 specimens

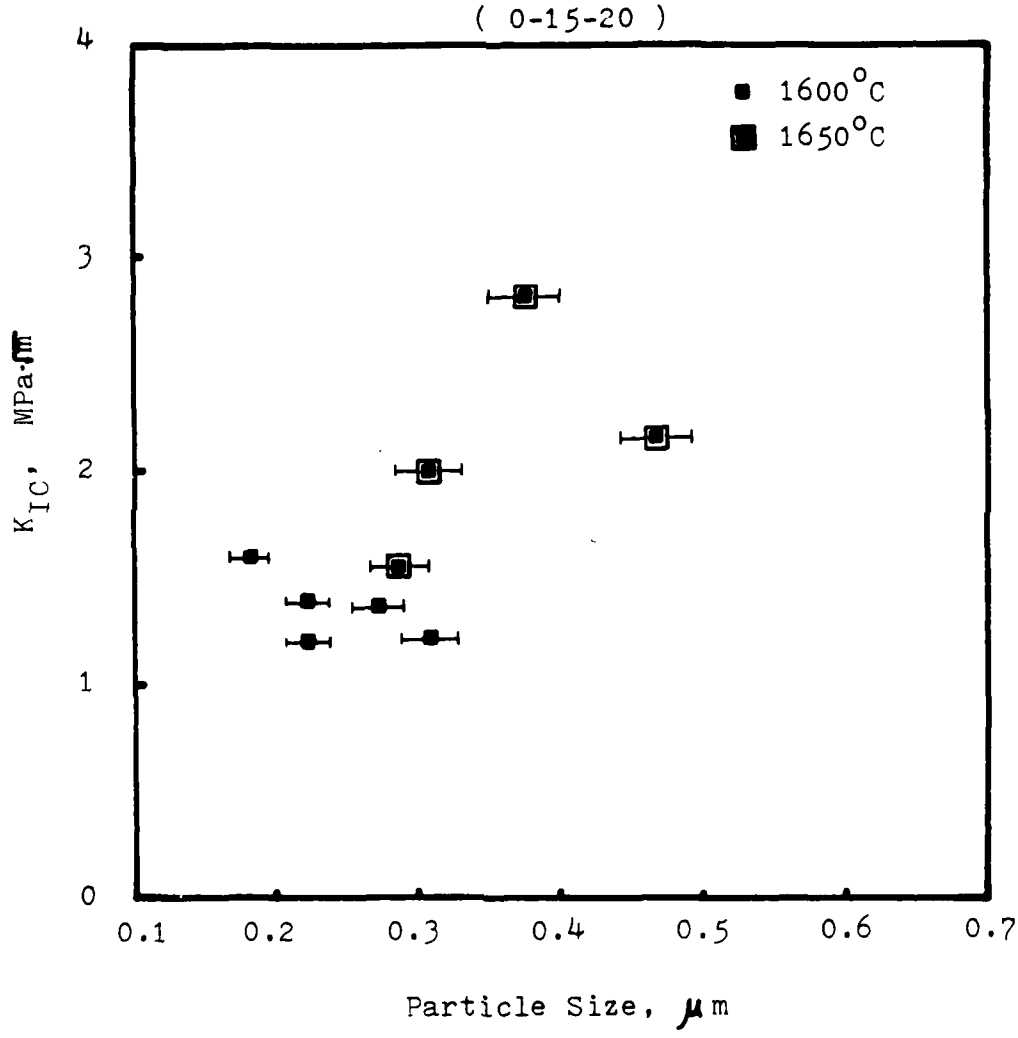

Fig. 9. K_{IC} vs. particle size changes in 0-15-20 specimens

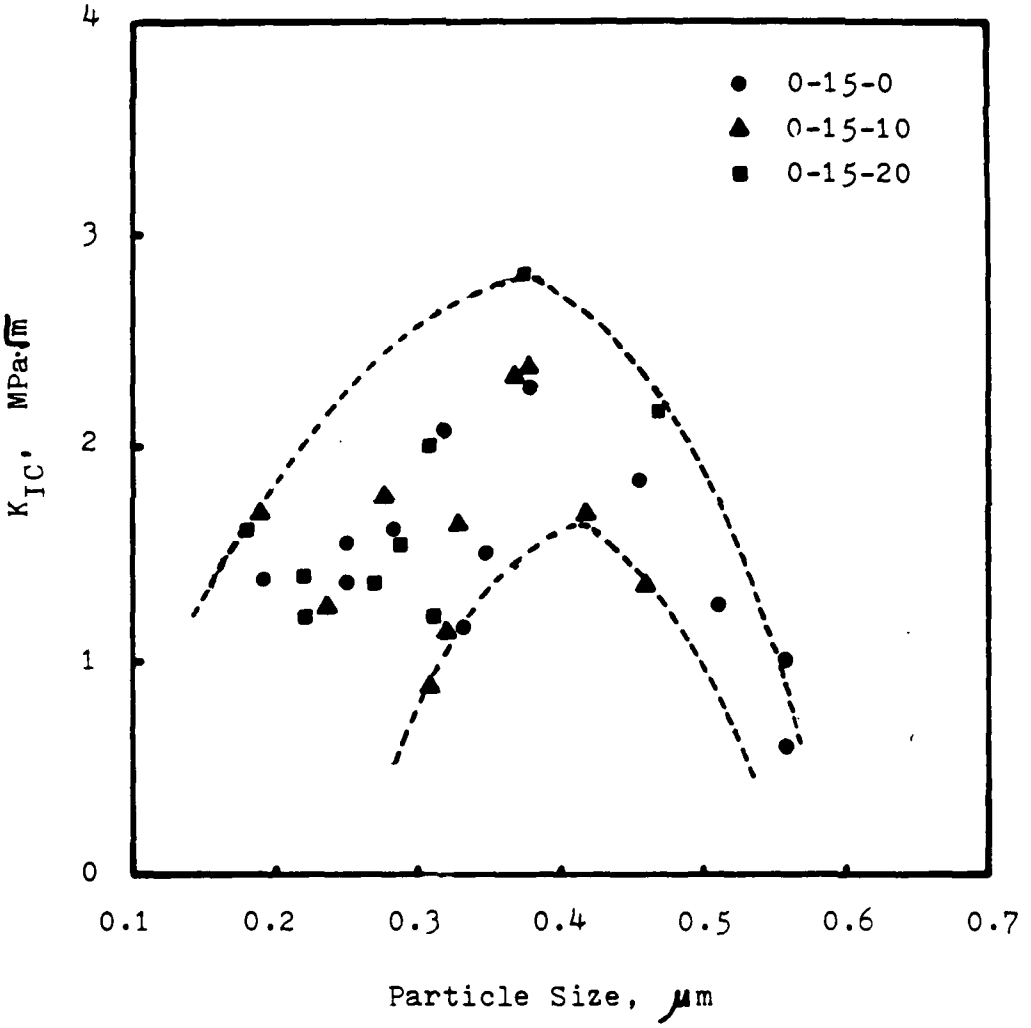

Fig. 10. K_{IC} vs. particle size changes in mullite system sintered at 1600°C and 1650°C.

DISTRIBUTION LIST

No. of Copies	To
12	Commander, Defense Technical Information Center, Cameron Station, Building 5, 5010 Duke Street, Alexandria, VA 22314
1	National Technical Information Service, 5285 Port Royal Road, Springfield, VA 22161
	Director, Defense Advanced Research Projects Agency, 1400 Wilson Boulevard, Arlington, VA 22209
1	ATTN: Dr. B. Wilcox
1	MAJ S. Wax
1	Dr. W. Snowdon
	Battelle Columbus Laboratories, Metals and Ceramics Information Center, 505 King Avenue, Columbus, OH 43201
1	ATTN: Mr. Winston Duckworth
1	Dr. D. Niesz
1	Dr. R. Wills
	Deputy Chief of Staff, Research, Development, and Acquisition, Headquarters, Department of the Army, Washington, DC 20301
1	ATTN: DAMA-PPP, Mr. R. Vawter
	Commander, Army Research Office, P.O. Box 12211, Research Triangle Park, NC 27709
1	ATTN: Information Processing Office
1	Dr. G. Mayer
1	Dr. P. Parrish
	Commander, U.S. Army Missile Command, Redstone Arsenal, AL 35898
1	ATTN: Technical Library
1	DRSMI-TB, Redstone Scientific Information Center
	Commander, U.S. Army Aviation Research and Development Command, 4300 Goodfellow Boulevard, St. Louis, MO 63120
1	ATTN: DRDAV-EGX
1	DRDAV-QE
1	Technical Library
	Commander, U.S. Army Tank-Automotive Command, Warren, MI 48090
1	ATTN: Dr. W. Bryzik
1	Mr. W. Wheelock
1	D. Rose
1	DRSTA-ZSK
1	DRSTA-UL, Technical Library
1	DRSTA-R
	Commander, U.S. Army Armament Materiel Readiness Command, Rock Island, IL 61299
1	ATTN: Technical Library
	Commander, U.S. Army Mobility Equipment Research and Development Command, Fort Belvoir, VA 22060
1	ATTN: DRDME-EM, Mr. P. Arnold
	Commander, U.S. Army Foreign Science and Technology Center, 220 7th Street, N.E., Charlottesville, VA 22901
1	ATTN: Military Tech, Mr. S. Mingledorf
	Director, Eustis Directorate, U.S. Army Mobility Research and Development Laboratory, Fort Eustis, VA 23604
1	ATTN: Mr. J. Robinson, DAVDL-E-MOS (AVRADCOM)
1	Mr. J. Lane
	Chief of Naval Research, Arlington, VA 22217
1	ATTN: Code 471
1	Dr. A. Diness
1	Dr. R. Pohanka
	Naval Research Laboratory, Washington, DC 20375
1	ATTN: Mr. R. Rice
	Headquarters, Naval Air Systems Command, Washington, DC 20360
1	ATTN: Code 5203
1	Code MAT-04JM
1	Mr. I. Macklin
	Commander, U.S. Air Force of Scientific Research, Building 410, Bolling Air Force Base, Washington, DC 20332
1	ATTN: Dr. B. Wilcox
	Commander, U.S. Air Force Wright Aeronautical Laboratories, Wright-Patterson Air Force Base, OH 45433
1	ATTN: AFWAL/MLLM, Dr. N. Tallan
1	AFWAL/MLLM, Dr. H. Graham
1	AFWAL/MLLM, Dr. R. Ruh
1	AFWAL/MLLM, Dr. A. Katz
1	AFWAL/MLLM, Mr. K. S. Mazdiyasni
1	Aero Propulsion Labs, Mr. R. Marsh
	National Aeronautics and Space Administration, Washington, DC 20546
1	ATTN: Mr. C. Bush
1	AFSS-AD, Office of Scientific and Technical Information
	National Aeronautics and Space Administration, Lewis Research Center, 21000 Brookpark Road, Cleveland, OH 44135
1	ATTN: J. Accurio, USAMRDL
1	Dr. H. B. Probst, MS 49-1
1	Mr. S. Dutta
	National Aeronautics and Space Administration, Langley Research Center, Hampton, VA 23665
1	ATTN: Mr. J. Buckley, Mail Stop 387
	Department of Energy, Division of Transportation, 20 Massachusetts Avenue, N.W., Washington, DC 20545
1	ATTN: Mr. Robert Schultz (TEC)
	Department of Transportation, 400 Seventh Street, S.W., Washington, DC 20590
1	ATTN: Mr. M. Lauriente
	National Bureau of Standards, Washington, DC 20234
1	ATTN: Dr. S. Wiederhorn
	National Research Council, National Materials Advisory Board, 2101 Constitution Avenue, Washington, DC 20418
1	ATTN: D. Groves
1	R. M. Spriggs
	Admiralty Materials Technology Establishment, Poole, Dorset BH16 6JU, UK
1	ATTN: Dr. D. Godfrey
1	Dr. M. Lindley
	AiResearch Manufacturing Company, AiResearch Casting Company, 2525 West 190th Street, Torrance, CA 90505
1	ATTN: Mr. K. Styhr
	AiResearch Manufacturing Company, Materials Engineering Dept., 111 South 34th Street, P.O. Box 5217, Phoenix, AZ 85010
1	ATTN: Mr. D. W. Richerson, MS 93-393/503-44
	AVCO Corporation, Applied Technology Division, Lowell Industrial Park, Lowell, MA 01887
1	ATTN: Dr. T. Vasilos
	Carborundum Company, Research and Development Division, P.O. Box 1054, Niagara Falls, NY 14302
1	ATTN: Dr. J. A. Coppola
	Case Western Reserve University, Department of Metallurgy, Cleveland, OH 44106
1	ATTN: Prof. A. H. Heuer
	Cummins Engine Company, Columbus, IN 47201
1	ATTN: Mr. R. Kamo
1	Dr. J. Patten
	Electric Power Research Institute, P.O. Box 10412, 3412 Hillview Avenue, Palo Alto, CA 94304
1	ATTN: Dr. A. Cohn
	European Research Office, 223 Old Marylebone Road, London, NW1 - 5the, England
1	ATTN: Dr. F. Roth
1	LT COL James Kennedy

No. of Copies	To
	Ford Motor Company, Turbine Research Department, 20000 Rotunda Drive, Dearborn, MI 48121
1	ATTN: Mr. A. F. McLean
1	Mr. A. Ezis
1	Mr. J. A. Mangels
1	Dr. R. Govila
1	Mr. R. Baker
	General Electric Company, Research and Development Center, Box 8, Schenectady, NY 12345
1	ATTN: Dr. R. J. Charles
1	Dr. C. D. Greskovich
1	Dr. S. Prochazka
	Georgia Institute of Technology, EES, Atlanta, GA 30332
1	ATTN: Mr. J. D. Walton
	GTE Laboratories, Waltham Research Center, 40 Sylvan Road, Waltham, MA 02154
1	ATTN: Dr. C. Quackenbush
1	Dr. W. H. Rhodes
	IIT Research Institute, 10 West 35th Street, Chicago, IL 60616
1	ATTN: Mr. S. Bortz, Director, Ceramics Research
	Institut fur Werkstoff-Forschung, DFVLR, 505 Porz-Wahn, Linder Hohe, Germany
1	ATTN: Dr. W. Bunk
	International Harvester, Solar Division, 2200 Pacific Highway, P.O. Box 80966, San Diego, CA 92138
1	ATTN: Dr. A. Metcalfe
	Kawecki Berylco Industries, Inc., P.O. Box 1462, Reading, PA 19603
1	ATTN: Mr. R. J. Longnecker
	Martin Marietta Laboratories, 1450 South Rolling Road, Baltimore, MD 21227
1	ATTN: Dr. J. Venables
	Massachusetts Institute of Technology, Department of Metallurgy and Materials Science, Cambridge, MA 02139
1	ATTN: Prof. R. L. Coble
1	Prof. H. K. Bowen
1	Prof. W. D. Kingery
	Midwest Research Institute, 425 Volker Boulevard, Kansas City, MO 64110
1	ATTN: Mr. Gordon W. Gross, Head, Physics Station
	Norton Company, Worcester, MA 01606
1	ATTN: Dr. N. Ault
1	Dr. M. L. Torti
	Pennsylvania State University, Materials Research Laboratory, Materials Science Department, University Park, PA 16802
1	ATTN: Prof. R. E. Tressler
1	Prof. V. S. Stubican
	RIAS, Division of the Martin Company, Baltimore, MD 21203
1	ATTN: Dr. A. R. C. Westwood
	Stanford Research International, 333 Ravenswood Avenue, Menlo Park, CA 94025
1	ATTN: Dr. P. Jorgensen
1	Dr. D. Rowcliffe
	State University of New York at Stony Brook, Department of Materials Science, Long Island, NY 11790
1	ATTN: Prof. Franklin F. Y. Wang
	United Technologies Research Center, East Hartford, CT 06108
1	ATTN: Dr. J. Brennan
1	Dr. F. Galasso
	University of California, Lawrence Livermore Laboratory, P. O. Box 808, Livermore, CA 94550
1	ATTN: Dr. C. F. Cline
	University of Florida, Department of Materials Science and Engineering, Gainesville, FL 32601
1	ATTN: Dr. L. Hench
	University of Newcastle Upon Tyne, Department of Metallurgy and Engineering Materials, Newcastle Upon Tyne, NEI 7 RU, England
1	ATTN: Prof. K. H. Jack
	University of Washington, Ceramic Engineering Division, FB-10, Seattle, WA 98195
1	ATTN: Prof. James I. Mueller
1	Prof. R. Bradt
	Westinghouse Electric Corporation, Research Laboratories, Pittsburgh, PA 15235
1	ATTN: Dr. R. J. Bratton
	Director, Army Materials and Mechanics Research Center, Watertown, MA 02172
2	ATTN: DRXMR-PL
1	DRXMR-PAT
1	DRXMR-K
10	DRXMR-MC

Army Materials and Mechanics Research Center
Watertown, Massachusetts 02172
TRANSFORMATION TOUGHENED CERAMICS -
A POTENTIAL MATERIAL FOR LIGHT DIESEL
ENGINE APPLICATIONS
T. Y. Tien
University of Michigan
Ann Arbor, Michigan 48109

Technical Report AMMRC TR 84-46, June 1984
54 pp.-illus.-tables, Contract DAAG 46-84-K-0001
Semi-annual Report - 1 October 1983 to March 31, 1984

AD__________

UNCLASSIFIED
UNLIMITED DISTRIBUTION

Key Words:
Heat Engine, Toughened Ceramic, Processing, Microstructure, Thermal Conductivity, Toughness, Zirconia, Alumina, Chromia, Hafnia, Mullite.

This report contains three parts: The mechanical behavior of composites in the system $Al_2O_3 \cdot Cr_2O_3/ZrO_2 \cdot HfO_2$ are presented in the first part of this report. The thermal conductivity studies of these compositions will be presented in the second part. The mullite - ZrO_2 system will be discussed in the third part. The results indicate that a composition containing 15 mole % of Cr_2O_3 in the matrix phase has a thermal conductivity comparable to that of stabilized zirconia. Composites heat treated at 900° and 1200°C for 400 hours showed no degradation in mechanical properties.

Army Materials and Mechanics Research Center
Watertown, Massachusetts 02172
TRANSFORMATION TOUGHENED CERAMICS -
A POTENTIAL MATERIAL FOR LIGHT DIESEL
ENGINE APPLICATIONS
T. Y. Tien
University of Michigan
Ann Arbor, Michigan 48109

Technical Report AMMRC TR 84-46, June 1984
54 pp.-illus.-tables, Contract DAAG 46-84-K-0001
Semi-annual Report - 1 October 1983 to March 31, 1984

AD__________

UNCLASSIFIED
UNLIMITED DISTRIBUTION

Key Words:
Heat Engine, Toughened Ceramic, Processing, Microstructure, Thermal Conductivity, Toughness, Zirconia, Alumina, Chromia, Hafnia, Mullite.

This report contains three parts: The mechanical behavior of composites in the system $Al_2O_3 \cdot Cr_2O_3/ZrO_2 \cdot HfO_2$ are presented in the first part of this report. The thermal conductivity studies of these compositions will be presented in the second part. The mullite - ZrO_2 system will be discussed in the third part. The results indicate that a composition containing 15 mole % of Cr_2O_3 in the matrix phase has a thermal conductivity comparable to that of stabilized zirconia. Composites heat treated at 900° and 1200°C for 400 hours showed no degradation in mechanical properties.

Army Materials and Mechanics Research Center
Watertown, Massachusetts 02172
TRANSFORMATION TOUGHENED CERAMICS -
A POTENTIAL MATERIAL FOR LIGHT DIESEL
ENGINE APPLICATIONS
T. Y. Tien
University of Michigan
Ann Arbor, Michigan 48109

Technical Report AMMRC TR 84-46, June 1984
54 pp.-illus.-tables, Contract DAAG 46-84-K-0001
Semi-annual Report - 1 October 1983 to March 31, 1984

AD__________

UNCLASSIFIED
UNLIMITED DISTRIBUTION

Key Words:
Heat Engine, Toughened Ceramic, Processing, Microstructure, Thermal Conductivity, Toughness, Zirconia, Alumina, Chromia, Hafnia, Mullite.

This report contains three parts: The mechanical behavior of composites in the system $Al_2O_3 \cdot Cr_2O_3/ZrO_2 \cdot HfO_2$ are presented in the first part of this report. The thermal conductivity studies of these compositions will be presented in the second part. The mullite - ZrO_2 system will be discussed in the third part. The results indicate that a composition containing 15 mole % of Cr_2O_3 in the matrix phase has a thermal conductivity comparable to that of stabilized zirconia. Composites heat treated at 900° and 1200°C for 400 hours showed no degradation in mechanical properties.

Army Materials and Mechanics Research Center
Watertown, Massachusetts 02172
TRANSFORMATION TOUGHENED CERAMICS -
A POTENTIAL MATERIAL FOR LIGHT DIESEL
ENGINE APPLICATIONS
T. Y. Tien
University of Michigan
Ann Arbor, Michigan 48109

Technical Report AMMRC TR 84-46, June 1984
54 pp.-illus.-tables, Contract DAAG 46-84-K-0001
Semi-annual Report - 1 October 1983 to March 31, 1984

AD__________

UNCLASSIFIED
UNLIMITED DISTRIBUTION

Key Words:
Heat Engine, Toughened Ceramic, Processing, Microstructure, Thermal Conductivity, Toughness, Zirconia, Alumina, Chromia, Hafnia, Mullite.

This report contains three parts: The mechanical behavior of composites in the system $Al_2O_3 \cdot Cr_2O_3/ZrO_2 \cdot HfO_2$ are presented in the first part of this report. The thermal conductivity studies of these compositions will be presented in the second part. The mullite - ZrO_2 system will be discussed in the third part. The results indicate that a composition containing 15 mole % of Cr_2O_3 in the matrix phase has a thermal conductivity comparable to that of stabilized zirconia. Composites heat treated at 900° and 1200°C for 400 hours showed no degradation in mechanical properties.

END

FILMED

4-85

DTIC